MEASUREMENT OF OPTICAL PARAMETERS OF THE EYE

AUTHOR

Prof. Earl L. Smith III: University of Houston

REVIEWER

Prof. Emeritus Barry L. Cole: University of Melbourne

INTRODUCTION AND OVERVIEW

This chapter includes a review of:

- Purkinje-Sanson images
- Axes and angles of the eye
- Corneal curvature: keratometry & corneal topography
  - Corneal contour measurements
  - Corneal topography
- Curvature of the surfaces of the lens: ophthalmophakometry
  - Calculations of the true radius of curvature
- Measurement of corneal thickness – pachymetry
- Axial length: x-rays and ultrasound
- Refractive indices of the optical media of the eye

1. PURKINJE-SANSON IMAGES

There are four major Purkinje images formed by the eye. The actual and apparent positions of the Purkinje images for a distant object are illustrated in Figures 2.1a and 2.1b. The position, size and attitude (i.e. erect or inverted) of a given image depend on the curvature of its reflecting surface.

Purkinje Image I

The first Purkinje image (designated '**I**') is formed by light reflected from the anterior surface of the cornea (actually the tear film) and is commonly referred to as the 'corneal reflex'. Since the anterior corneal surface is essentially a convex mirror, the image formed by an object at infinity will be virtual, erect, and appear to be located in the anterior portion of the lens.

Purkinje Image II

The second Purkinje image (**II**) is formed by light reflected from the posterior surface of the cornea. The image is virtual and erect, but it is slightly smaller than image **I**. It appears to be slightly in front of image **I**. In reality, image **II** is formed slightly behind image **I**, but since light from image **II** undergoes refraction at the anterior surface of the cornea, it appears slightly closer to the front of the eye. The apparent image is also slightly larger than the true catoptric image.

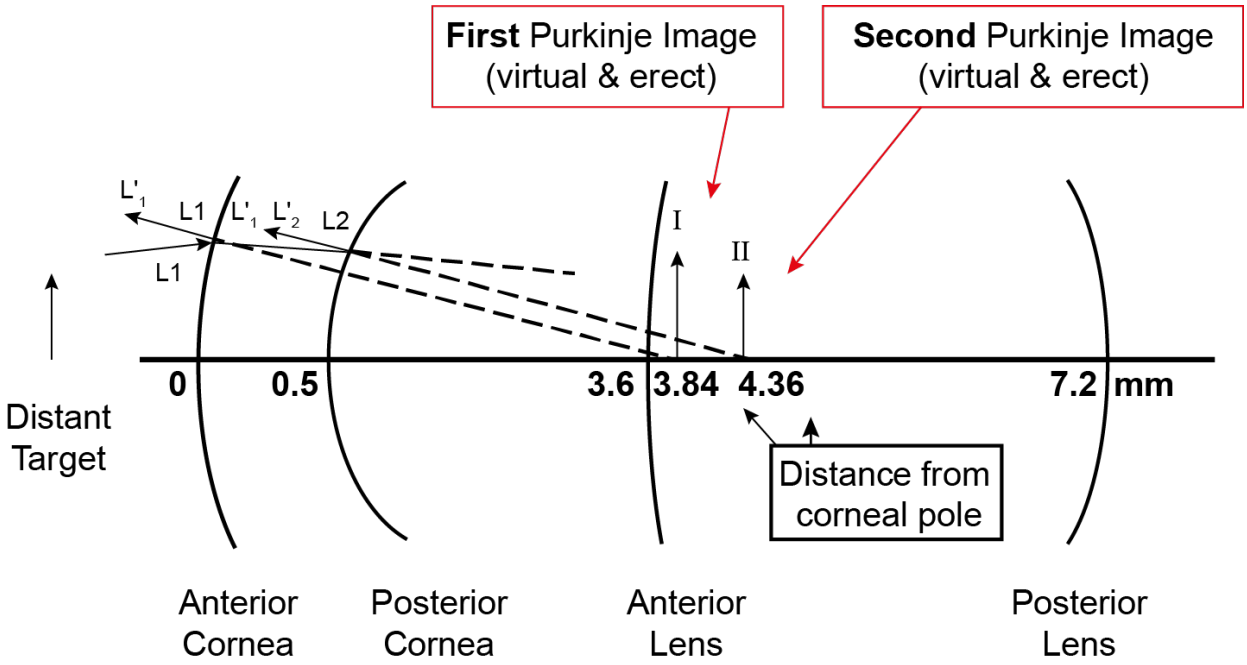

Figure 2.1a: *Purkinje-Sanson Images (I and II)*

Note: For a distant object, the size of the image formed by a spherical mirror is directly proportional to the radius of curvature of the reflecting surface. The fact that image **II** is smaller than image **I** tells you that the radius of curvature of the posterior surface of the cornea is shorter than the radius for the anterior surface.

Purkinje Image III

The third Purkinje image is formed by reflection at the anterior surface of the lens. The image is virtual and erect. In the unaccommodated eye it is about twice as large as image **I** and it appears to be located in the vitreous. With an increase in positive accommodation the size of the image decreases and it appears to move forward. The changes in image **III** reflect the changes in lens shape that take place during accommodation; specifically, the fact that the radius of the anterior surface gets shorter during positive accommodation.

Purkinje Image IV

The fourth Purkinje image is formed by reflection at the posterior surface of the lens. The posterior surface acts as a concave mirror, as a result, image **IV** is real and inverted. In the unaccommodated state, image **IV** is the smallest Purkinje image and it appears to be located approximately in the plane of image **I**. When the eye accommodates, image **IV** gets slightly smaller and moves slightly closer to the posterior of the lens. However, the changes observed for image **IV** during accommodation are smaller than those associated with image **III**, i.e. the posterior surface radius changes less than the radius for the anterior surface.

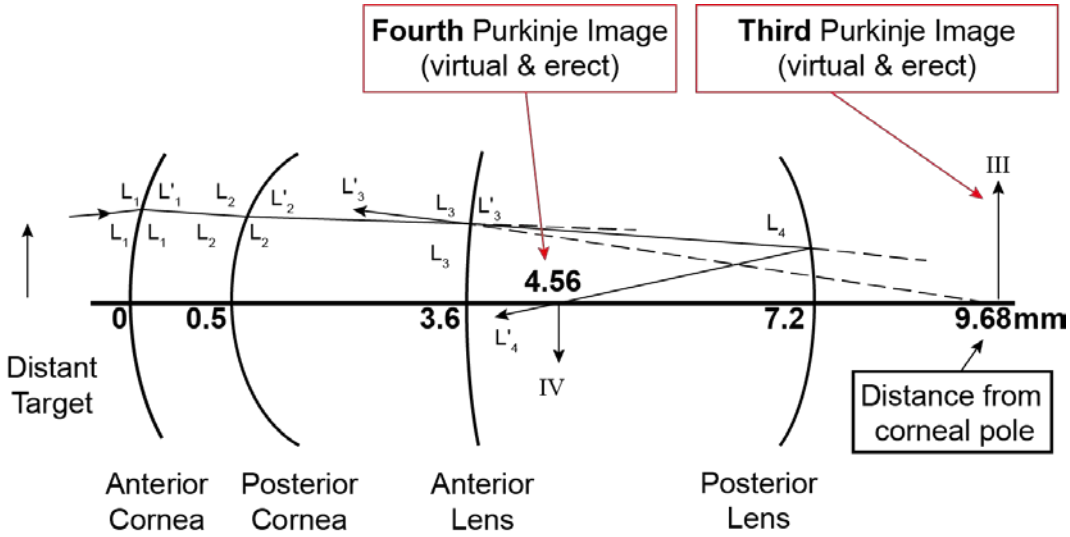

Figure 2.1b: *Purkinje-Sanson Images (III and IV)*

COMPARISON OF PURKINJE IMAGES

Relative Sizes

Unaccommodated eye	**III** > **I** > **II** > **IV**
Accommodated eye (about 10 D)	**I** > **II** > **III** > **IV**

The change in position noted is that III moves closer to the cornea and IV moves closer to the retina.

Brightness

There are substantial differences in the apparent brightness of these images. The first Purkinje image is approximately 100X brighter than the second image. The second Purkinje image is just slightly brighter (about 20%) than the third and fourth images which are about equally bright. These differences in brightness are due to three factors:

1. The primary reason for these differences in brightness is that the proportion of light reflected from an interface is dependent on the difference in the indices of refraction between the two media forming the interface; the greater the difference in the indices of refraction, the greater the proportion of light reflected. Fresnel's formula can be used to calculate the proportion of light reflected at an interface for light that strikes the interface in a perpendicular manner.

Fresnel's Formula:

Reflectance = $(n' - n)^2 / (n' + n)^2$

Where n and n' represent the indices of refraction of the first and second media, respectively.

Example: For a beam of light incident normally on the cornea, what proportion of light is reflected by the tear film?

$n_{(tears)} = 1.336$; $n_{(air)} = 1.0$

Reflectance (R) = $(1.336 - 1.0)^2 / (1.336+1.0)^2$
= 0.0207 (about 2.0%)

Example: Consider how much of the incident light would be reflected to form the second Purkinje image.

$n_{(aqueous)} = 1.336$; $n_{(cornea)} = 1.376$

Reflectance (R) = $(1.336-1.376)^2 / (1.336+1.376)^2$
= 0.000217 (i.e. 0.02%)

2. Differences in the reflecting qualities of the various interfaces contribute to brightness differences. For example, the tear film provides a relatively smooth surface where light is reflected primarily in a specular manner. In comparison, the surfaces of the lens are not as optically smooth and light is reflected in both a diffuse (i.e. scattered) and specular manner.

3. Only the first Purkinje image is formed by reflection alone. Light associated with the other images undergoes refraction (and reflection and absorption) both before and after reflection by their respective interfaces (i.e. the apparent images are actually cata-dioptric-images).

Motion of the Purkinje Images

If the light source producing the Purkinje images is moved perpendicular to the optical axis of the eye, the Purkinje images will move. The first, second, and third Purkinje images are erect and, therefore, will appear to move in the same direction as the light. However, since the fourth Purkinje image is inverted, it demonstrates 'against' motion.

OTHER CATOPTRIC IMAGES

Since Purkinje's time (about 1823), other catoptric images have been described. For example, although we assumed that the index of refraction of the crystalline lens was uniform, that is not the case. In reality, the index of refraction increases from the surface of the lens (the cortex) to the centre of the lens (the nucleus). In many cases (especially in older patients), relatively large changes in index occur over a relatively short distance. In essence, the crystalline lens can be effectively represented as a biconvex lens within a biconvex lens. As a result, two catoptric images formed by reflection at the anterior and posterior surfaces of the nucleus of the lens have been described. In general, these are relatively indistinct and cannot be consistently observed.

Another class of catoptric images are called Second Order images. All of the Purkinje-Sanson images which have been discussed thus far are First Order images, which means that they are formed by a single reflection. Second order images are formed by reflection at two interfaces within the eye. There are two major second order catoptric images that have been described. One of these images is formed by light reflected by the anterior surface of the lens and then by reflection at the anterior surface of the cornea. This image, which is sometimes referred to as the fifth Purkinje image (**V**), is real and formed near the posterior lens surface. The other important second order image is formed by reflection at the posterior surface of the lens and again by reflection at the anterior surface of the cornea. It is often referred to as the sixth Purkinje image (**VI**). It is also real, but it is formed closer to the retina than the fifth image. In contrast to first order catoptric images that are formed by light reflected out of the eye, the second order images, in particular the **VI** image, can under certain conditions be seen by the subject (e.g. during direct ophthalmoscopy).

In general, **ocular** catoptric images, even second order images, do not produce any visual disturbances. However, some spectacle wearers do see second order catoptric images formed by reflection from the posterior and anterior surfaces, respectively, of their spectacle lenses.

The most common uses of Purkinje Images:

1. Locating axes and their associated angles in the eye
2. Measuring corneal curvature (keratometry, image **I**)
3. Measuring lens changes in accommodation
4. Measuring lens position and curvature
5. Measuring eye position and eye movements.

2. AXES AND ANGLES OF THE EYE

AXES

1. **Optical Axis:** The line connecting the centres of curvature of all of the refracting surfaces. It is perpendicular to all refracting surfaces.
2. **Visual Axis:** The line that connects the fixation point and the fovea and that passes through the nodal points (actually the visual axis is composed of two line segments; the line from the fixation point to the primary (first) nodal point and the line from the secondary nodal point to the fovea).
3. **Pupillary Axis:** The line from the centre of the entrance pupil (the image of the real pupil formed by refraction at the cornea) that intersects the cornea in a perpendicular manner.
4. **Line of Sight:** The line from the centre of the entrance pupil to the object of regard (i.e. the fixation point).
5. **Fixation Axis:** The line from the fixation point to the centre of rotation of the eye (an imaginary point about 14mm behind the cornea; it is an important reference point for eye movements).

ANGLES

1. **Angle Alpha:** The angle between the optical axis and the visual axis formed at the nodal point.
2. **Angle Kappa:** The angle between the pupillary axis and the visual axis.
3. **Angle Lambda:** The angle between the line of sight and the pupillary axis formed at the centre of the entrance pupil.
4. **Angle Gamma:** The angle between the fixation axis and the optical axis.

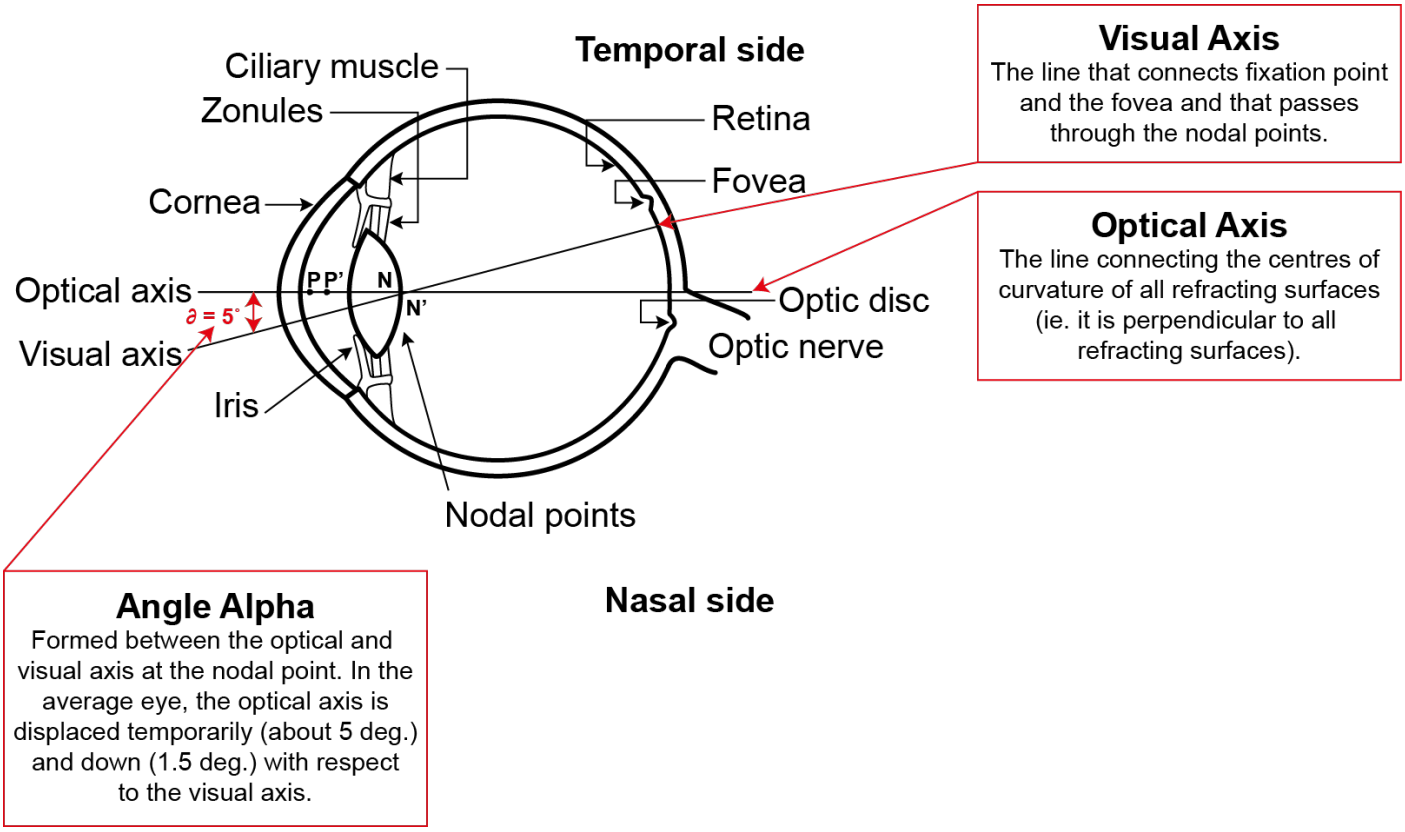

Figure 2.2: *Visual Axis, Optical Axis, Angle Alpha*

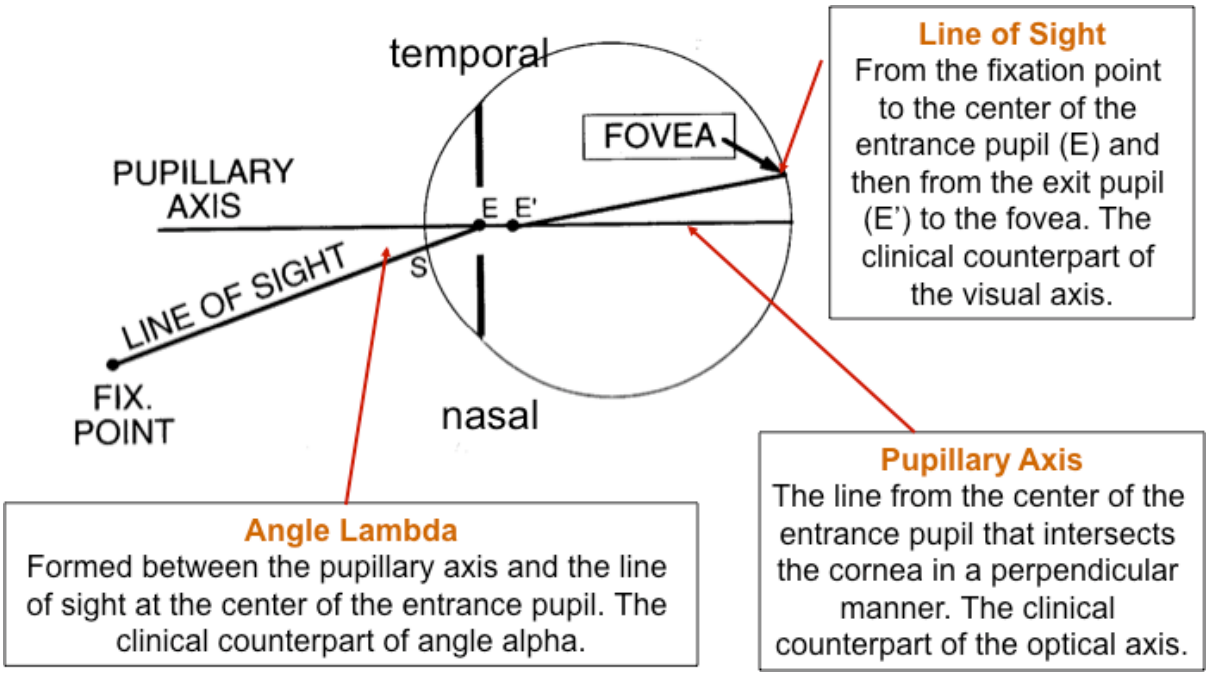

Figure 2.3: *Line of Sight, Pupillary Axis, Angle Lambda*

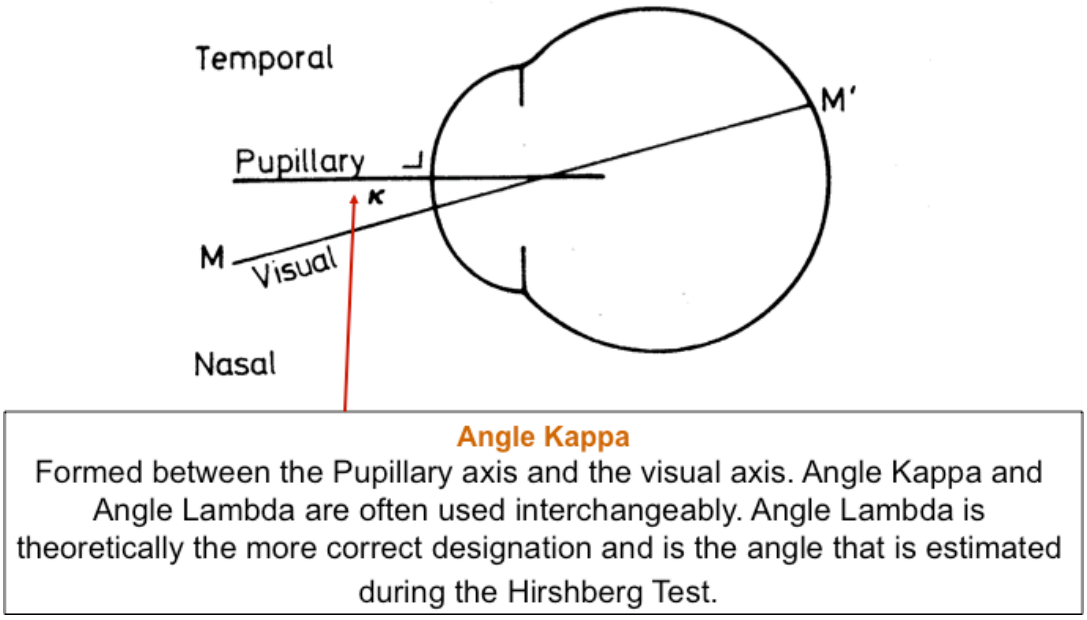

Figure 2.4: *Angle Kappa*

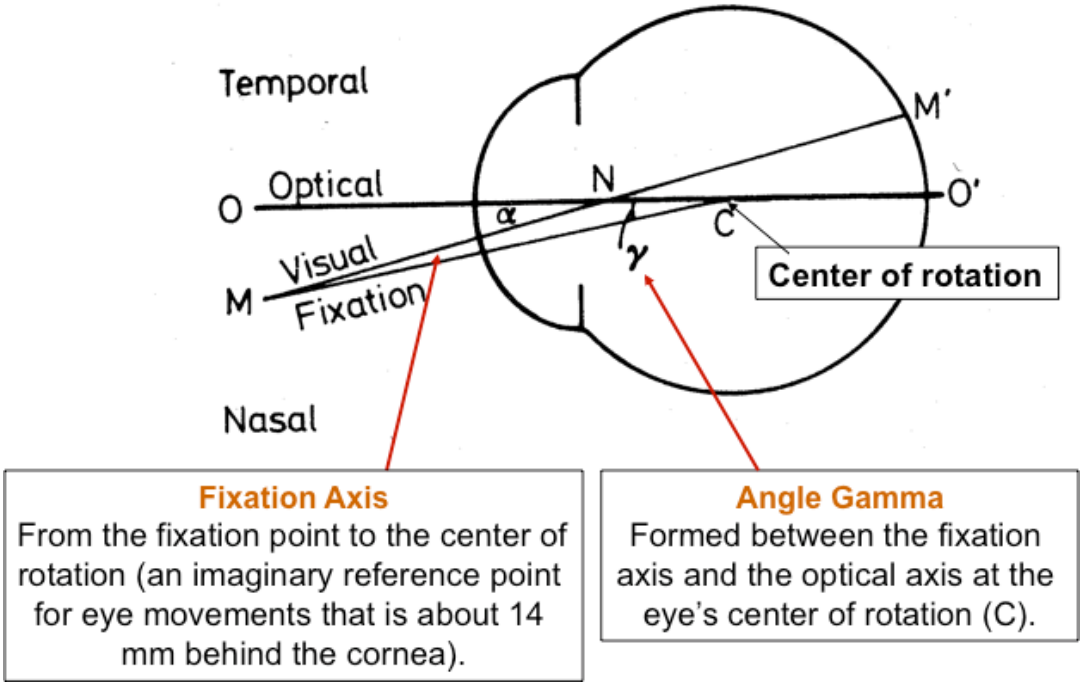

Figure 2.5: *Fixation Axis, Angle Gamma*

The following acronym may help you remember the various axes and the included angles (Figure 2.6).

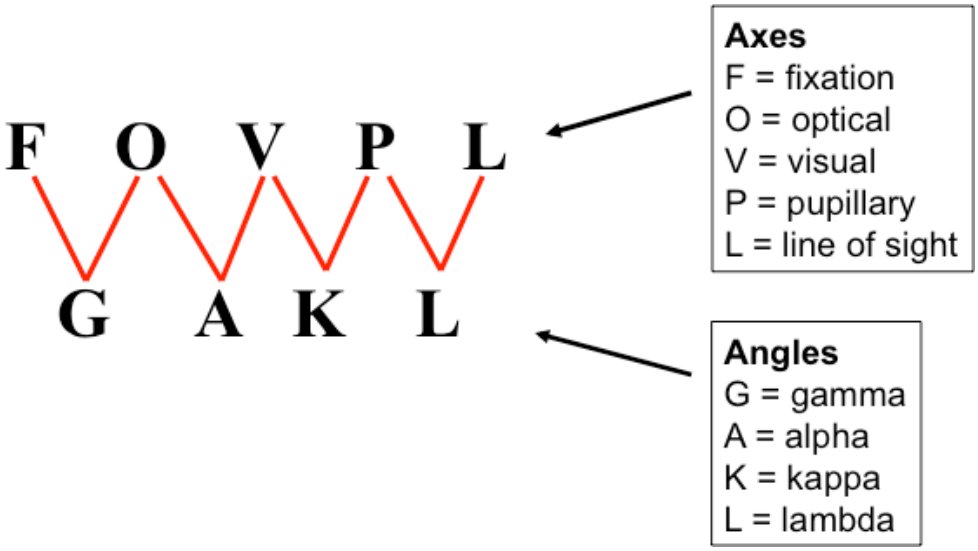

Figure 2.6: *Acronym of the visual axes and their corresponding angles*

If the eye had a true optical axis, a light source could be positioned in such a manner that when you were looking over the light source at the eye, all of the Purkinje images would be superimposed. This position of the light would have to be on the optical axis since only a beam of light traveling along the optical axis would intersect all of the refracting surfaces of the eye in a perpendicular manner and, thus, be reflected back along the optical axis at each interface (i.e. resulting in an apparent superimposition of the reflected images). However, it is impossible to position a light source to superimpose all of the catoptric images which clearly illustrates that the eye does **not** have a true optical axis.

It is possible to position a light so that the four Purkinje images nearly superimpose, but interestingly, the light will not correspond to the subject's fixation point and the line from the light through the images does not intersect the retina at the fovea, i.e. the visual axis of the eye must not coincide with the approximate optical axis of the eye. In general, the optical axis is displaced temporally (about 5 deg) and down (about 1.5 deg) with respect to the visual axis. Since the optical and visual axes both go through the nodal point, angle alpha is formed between them at the nodal point. By convention, angle alpha is positive when the visual axis is nasal to the optic axis. If the visual axis intersects the cornea temporal to the optic axis, then angle alpha is negative. Angle alpha must be taken into account in order to properly interpret the results of the **Hirshberg test** of interocular alignment (an illustration of how the test can be used to diagnose strabismus is included below in Figure 2.7).

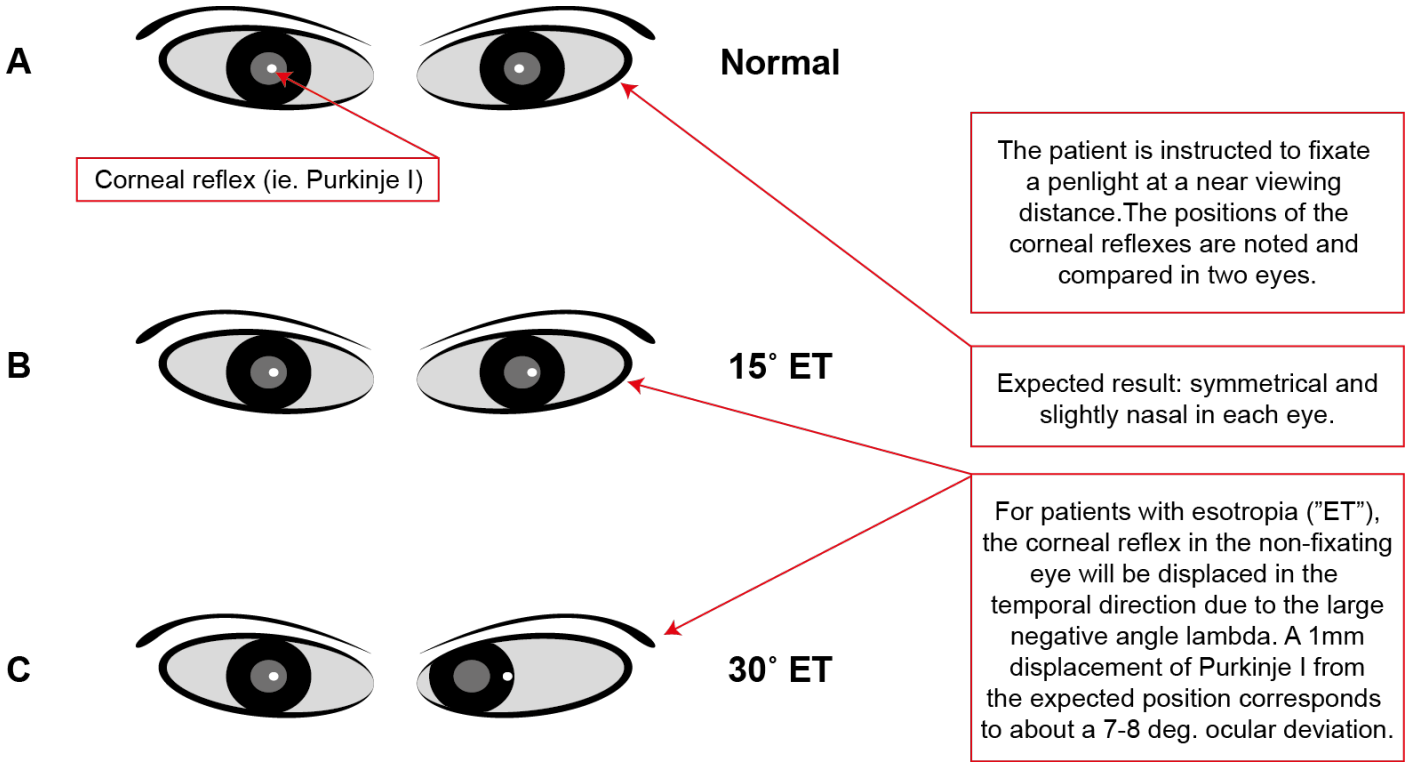

Figure 2.7: *Hirschberg Test of Interocular Alignment*

Angle alpha is clinically important because it provides some insight into the fixation characteristics of your patients. But, we cannot measure angle alpha in a clinical situation because it is not possible to locate the nodal point. To overcome this problem, two additional axes were defined that represent the clinical counterparts to the optical axis and the visual axis. The clinical counterpart of the optical axis is the pupillary axis. It is easily identified in the clinic using catoptric images. A light source simply has to be positioned so that the first Purkinje image is centred in the entrance pupil (i.e. the line from the light to the centre of the entrance pupil must be perpendicular to the cornea). The line of sight is the clinical counterpart of the visual axis. Thus, angle lambda, which is formed in the centre of the entrance pupil, is the clinical counterpart of angle alpha and the angle which is estimated during the Hirshberg Test. Angle lambda is positive when the line of sight is nasal relative to the pupillary axis.

Note: In many texts the Hirshberg test is said to provide an estimate of angle kappa. However that is not the case. In fact, the visual axis and the pupillary axis may not intersect to form an angle since in most individuals the visual axis does not go through the centre of the entrance pupil. Nevertheless, the term angle kappa and angle lambda are often (but incorrectly) used in an interchangeable manner.

Figure 2.7(above) shows where the first Purkinje image will appear when a patient with normal fixation looks at a small light source. Basically, this diagram illustrates the optics of the Hirshberg test. The light source, since it is the fixation point, will fall on the patient's line of sight which, as illustrated, normally intersects the cornea nasal to the pupillary axis (i.e. the patient has a positive angle lambda). To locate the approximate position of the corneal reflex, consider a ray from the light source that intersects the cornea in a perpendicular manner and passes through the cornea's centre of curvature. Since this ray is perpendicular to the cornea, light from this ray that is reflected at the anterior corneal surface will be reflected in a perpendicular manner (i.e. straight back toward the light source) forming the first Purkinje image. So, if you are positioned behind the light source and looking at your patient's eye, the corneal reflex will be located somewhere along this ray. Its exact position depends on the radius of curvature of the cornea (and thus, the location of the reflecting focal point of the anterior cornea) and how far away the light source is from the patient. But, for most reasonable near fixation distances, it will be located slightly in front of the cornea's reflecting focal point (i.e. 1/2 the radius of curvature). It is important to note that the cornea's centre of curvature is behind the centre of the eye's entrance pupil. As a consequence, the first Purkinje image is normally formed on the nasal side of the centre of the entrance pupil (as shown in Fig. 2.8). For most individuals the corneal reflex will appear to be about 0.5 mm nasal to the centre of the pupil.

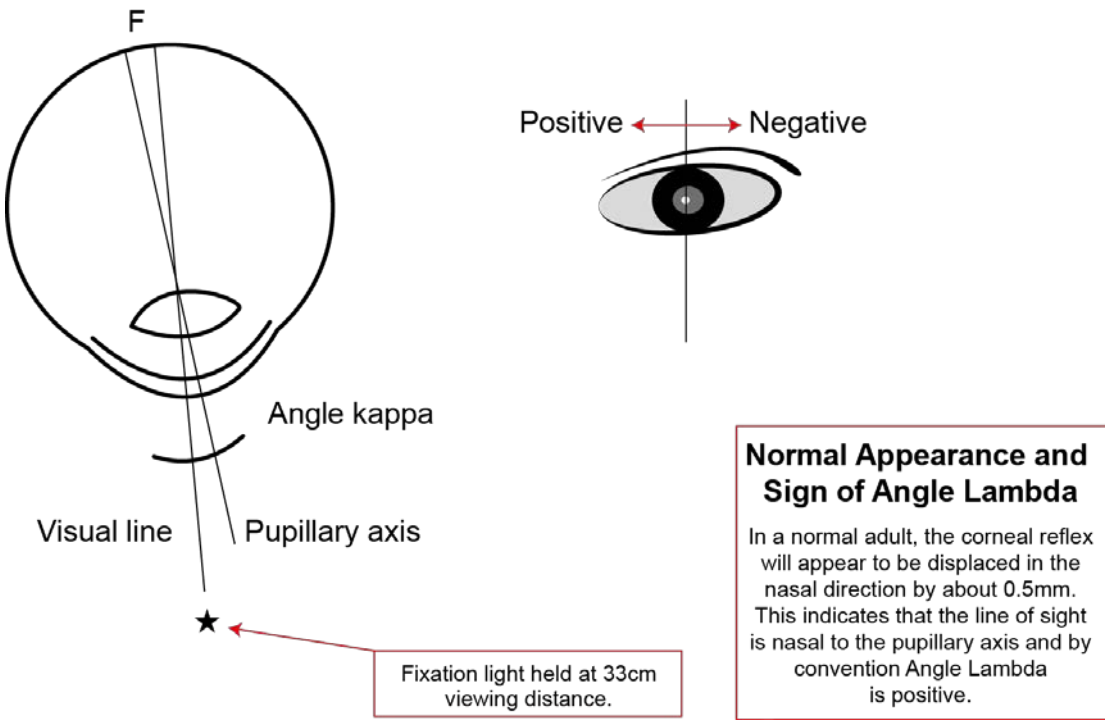

Figure 2.8: *Normal appearance and sign of angle lambda*

In the above example, a number of factors can influence the relative position of the corneal reflex relative to the centre of the entrance pupil (Figure 2.9). Of primary interest is angle lambda. The displacement of the corneal reflex from the centre of the entrance pupil increases as angle lambda increases in magnitude. Its exact position is also influenced by:

1. The radius of curvature of the cornea,
2. The fixation distance, and in some cases,
3. Pupil size

(Since the pupil may not constrict/dilate in a symmetrical manner, the absolute position of the centre of the entrance pupil can change with pupil size).

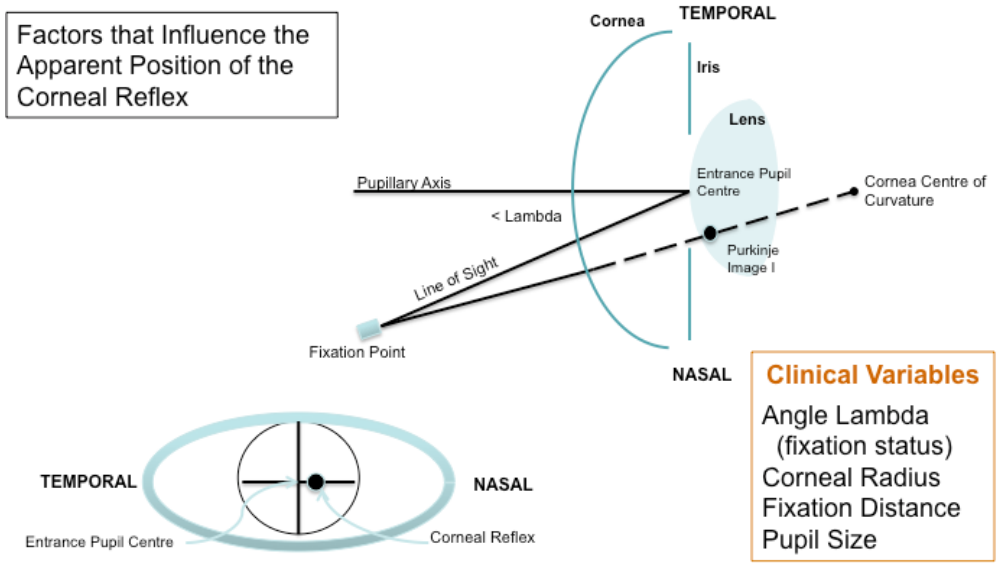

Figure 2.9: *Factors that influence the apparent position of the corneal reflex*

3. CORNEAL CURVATURE: KERATOMETRY AND CORNEAL TOPOGRAPHY

KERATOMETRY

Keratometry (Kerato = denoting the cornea; metry = to measure) is the measurement of the radius of curvature of the anterior corneal surface. Frequently, the term 'ophthalmometry' (which historically is the more correct term) is used as a synonym for keratometry.

Since it is not possible to physically measure the cornea in a convenient and non-invasive manner (at least in a living eye), clinicians are determining the radius of curvature of the anterior corneal surface indirectly. In essence, the cornea is treated as a convex mirror and its physical characteristics are calculated using information obtained from the catoptric images formed by the anterior corneal surface (Figure 2.10).

Note: Catoptric images are images formed by reflection; dioptric images are images formed by refraction.

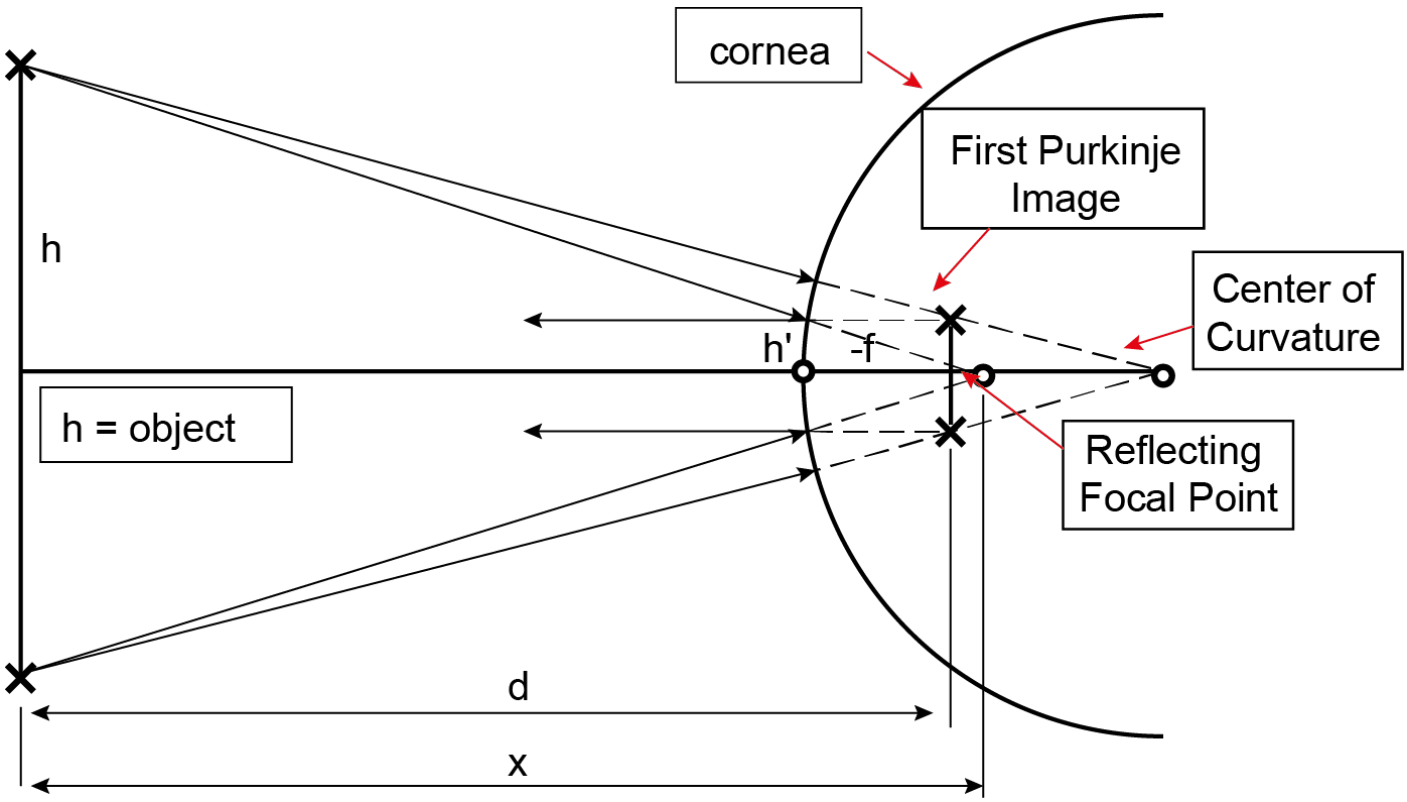

Figure 2.10: *Principles of keratometry using the first Purkinje image*

The catoptric image formed by reflection at the anterior corneal surface is known as the 'corneal reflex' or the 'First Purkinje Image'. To measure curvature, investigators took advantage of the following relationship: For a given object and object distance, the size of the image formed by a **spherical** mirror varies with the curvature of the reflecting surface. Since the cornea can be treated as a convex mirror, its radius of curvature can be calculated by measuring the size of the reflected image produced by an object of known size. The relationship between the object and image used in keratometers to determine radius of curvature was derived as follows (Fig. 2.11).

Let AB represent the object. The position of the image can be determined by construction. A ray AC passing from the object to the centre of curvature (C) strikes the cornea in a perpendicular manner and is reflected back on itself. A ray AF directed toward the focal point (F; Note: the focal point representing the **reflecting** characteristics of the surface, not the **refracting** characteristics) strikes the cornea at M and is reflected parallel to the optical axis (BC). The intersection of the projections of these rays represents the image of A which is labeled 'D'. Actually the image of AB will be curved (it will be slightly concave toward C), but we can ignore this and consider the image to be perpendicular to the axis. The image of B is labeled 'E'.

The points E and F are very close to each other and without inducing a serious error we can consider E and F to be the same point (obviously this assumption becomes more valid as the object distance is increased). With this assumption, DEM can be considered a triangle that is similar to triangle ABF. Therefore:

$$DE/AB = DM/BF$$

Since E and F are considered to be the same point, DM can be considered to be equal to the focal length of the mirror (remember f = r/2).

$$DE/AB = f/BF = r/2(BF)$$

Solving for r:

$$r = \frac{2(BF)(DE)}{AB}$$

In other words:

$$r = \frac{2(\text{object to image distance})(\text{image size})}{\text{object size}}$$

This equation is sometimes referred to as the **'keratometer formula'**.

In clinical instruments (e.g. the B & L Keratometer) an object of known size (the lighted mires) is attached to a short-focus telescope system that has a small depth of field. By viewing the image through the telescope, the distance BF (i.e. the object to image distance) and the size of the object (AB) are held constant. The keratometer is then used to measure the image size (DE) and to calculate the radius of curvature. The errors introduced by assuming that DM = f and that E and F are the same point are less than 0.1 D. However, a 1.0% error in the object-image distance will induce a measurement error of about 0.8 to 0.9 D. (What happens if the keratometer is not focused properly?).

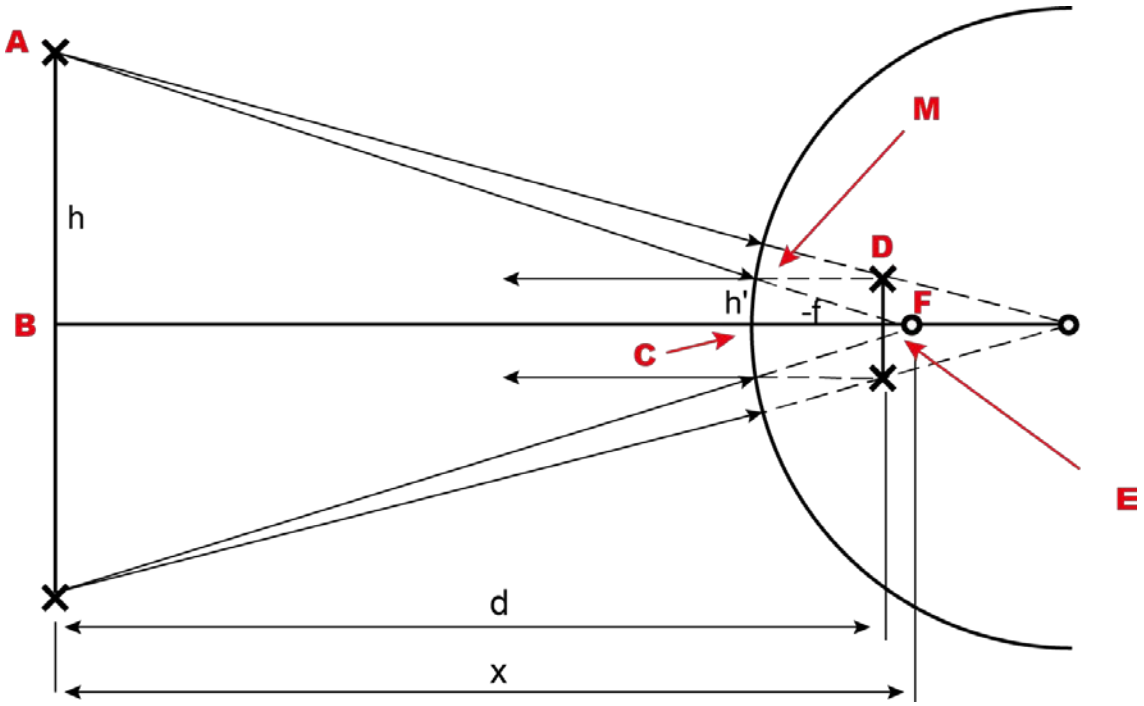

Figure 2.11: *The keratometry formula*

MEASUREMENT OF IMAGE SIZE

Direct and accurate measurements of the size of the corneal reflex are difficult because it is impossible to voluntarily immobilize the eye. Even during attempted steady fixation, the eye is never perfectly still [instead it manifests small drift movements, micro-saccades (small flick-like movements), and fixation tremors]. Since the image produced by a mirror is rotated through an angle twice as large as the rotation of the mirror, even these small eye movements prevent direct measurements from being accurate. To overcome this difficulty, vision scientists borrowed an idea from early astronomers and introduced a doubling device into the keratometer's telescope system. Through the doubling device, the observer sees two images of the corneal reflections separated from one another by a certain distance. With the doubling system, the reflected images are still moving, however, the relative separation between the 'double' images does not change as the eye moves. As a result, if the displacement produced by the doubling device is accurately calibrated, it is then possible to adjust the relative image displacement until the image is displaced by an amount equivalent to its diameter. Obviously, if you know the amount of optical displacement that is required to move an image a distance equivalent to its diameter, you have, in fact, measured its diameter.

There are two basic types of doubling systems used in clinical instruments:

1. Variable Doubling Systems

Helmholtz perfected the variable doubling system. The majority of commercially available keratometers and ophthalmometers (e.g. the B&L Keratometer) use a type of variable doubling system (different manufacturers produce the doubling in different ways). A simplified diagram of the doubling system used in the B&L Keratometer is illustrated in Figure 2.12. Light from the cornea is divided into several bundles by apertures at the telescope objective. Positioned behind one aperture is a moveable 'base-in' (or base-down) prism. Without the prism in place the light passing through the different apertures would come to a focus in the same plane and form a single image. The prism deviates a portion of this light to form a second image in the same image plane. Movement of the prism back and forth alters the effective power of the prism and, thus, increases or decreases the doubling in the image plane. When it is positioned so that the displacement is equal to the mire image size, the crosses (or minus signs), which are the ends of the image, will coincide.

From your experiences with the B&L Keratometer, you know that when the corneal image is in focus, there are three images. That is because the keratometer doubles the image in two meridians at once. The doubling in two meridians allows curvature to be measured in both meridians simultaneously. Instruments like the B&L Keratometer that are

designed to measure both principal meridians simultaneously are called ‘one position’ instruments. Many ophthalmometers (e.g. the old A.O. Ophthalmometer and the new Haig-Strait Ophthalmometer) contain a single doubling system that must be rotated to measure the second meridian. These ophthalmometers are referred to as ‘two position’ instruments.

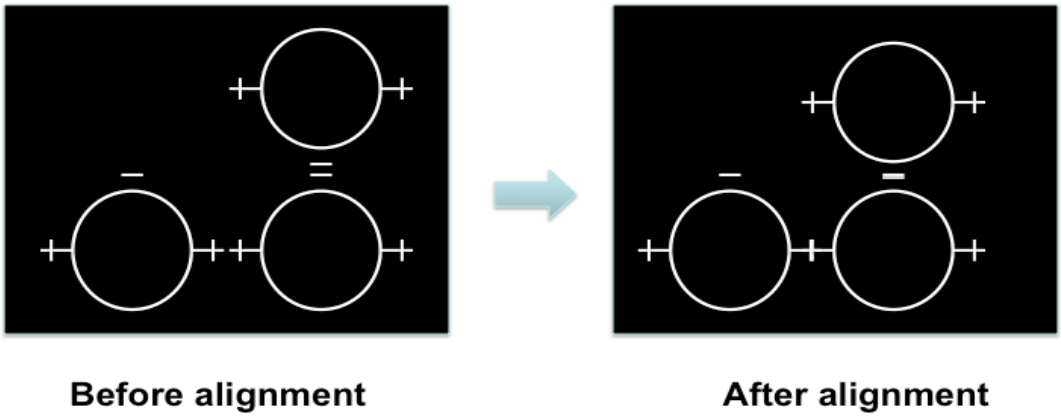

Figure 2.12: *Diagram of keratometer mires in variable doubling system*

2. Fixed Doubling Systems

Javal and Schiotz developed the fixed doubling system. In most ophthalmometers (e.g. the Universal Ophthalmometer) that use this system the image is doubled with a Wollaston prism. A Wollaston prism consists of two quartz prisms cemented together (apex to base) to form a thick plate. Since the prisms are cut in different directions with respect to the axes of the quartz crystal, the combination is doubly refracting. As a result, two images are formed that are separated by a fixed amount. In order to align the images properly with this type of system, it is necessary to vary the size of the object, i.e. with this system, the image size and object distance are held constant and the **size** of the object required to produce a given image is measured (see Fig. 2.13). The Haig-Streit Ophthalmometer, one of the better instruments available today, employs this type of doubling system. Instruments with fixed doubling systems are usually two-position instruments.

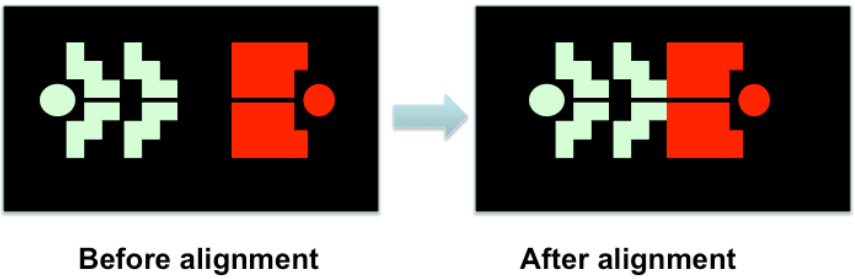

Figure 2.13: *Diagram of opthalmometer mires in a fixed doubling system*

SCHEINER FOCUSING SYSTEM

Since maintaining a specific and constant object-image distance is critical for accurate keratometry, instrument designers have employed a Scheiner focusing system (a.k.a. a ‘coincidence’ focusing system) to facilitate accurate positioning of the instrument. The key to a Scheiner focusing system is that the subjective end-point is based on whether the target is single vs. double. With more traditional focusing systems, the observer adjusts the instrument until the object of regard appears to be clear. However, your ability to detect doubling is better than your ability to detect blur. Consequently, you are able to focus an instrument more accurately using a Scheiner system.

A Scheiner focusing system includes an opaque disc that has two apertures in it (a Scheiner disc). In this example, the object consists of a single point source (you can consider it to represent a single point of the corneal reflex

produced by the keratometer's mires). Light leaving the point is restricted to two bundles of light by the two apertures in the Scheiner disc. After passing through these apertures, the light from the point source encounters a focusing lens which converges the light to the 'in focus' plane (Fig. 2.14).

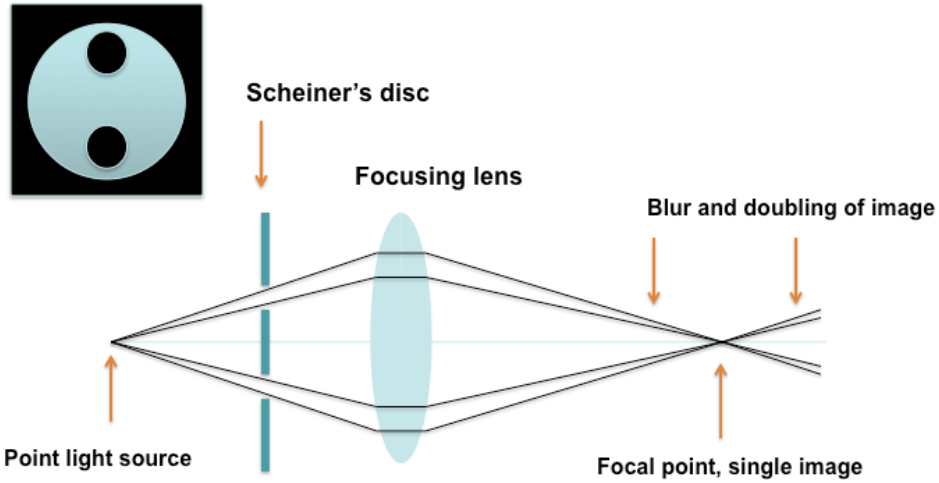

Figure 2.14: *The Scheiner's disc focussing system creates image doubling outside of the focal plane*

Note: The presence of the Scheiner disc does not affect the vergence of the light or effective power of the lens.

Consider what the image of the point would look like if you placed an image screen in the 'in focus' plane. It would look like a single point image. However, if the image screen was placed too near to or too far from the focusing lens (in the 'out of focus' positions), the image of the point source would consist of two images, both of which would be slightly out of focus. The closer the image screen gets to the 'in focus' plane the closer the two images get to each other until they form a single image in the 'in focus' plane. It is important to realize that the same thing would happen to the image if the image screen were fixed in position in the 'in focus' plane and the focusing lens and Scheiner disc were moved closer to the point object. Assuming that the distance from the image screen and focusing lens was fixed, you would see the image go from single to double. This is analogous to how you focus the keratometer. With the B & L Keratometer, the observer focuses the eyepiece so the crosshairs are in focus.

Note: The crosshairs correspond to the desired 'plane of focus' inside the keratometer.

Next, the patient is properly aligned and the entire keratometer is moved either closer or farther away from the patient while the observer watches the bottom right-hand pair of rings. As you move the instrument in and out (i.e. as you focus the instrument in and out), the separation of the rings changes. When the instrument is properly focused, the image of the mires will be formed in the 'plane of focus' of the eyepiece and they will be single. This is a very critical step because it establishes the appropriate object-image distance. The Scheiner focusing system makes you very sensitive to very small degrees of defocus.

TARGET OF KERATOMETER MEASUREMENT

Although we would like to have an instrument that would determine the true shape of the cornea, the keratometer clearly does not measure the true corneal shape. The keratometer simply measures the size of the first Purkinje image. From this measurement the curvature of the cornea is calculated. However, it is important to realize that the formulas that are used to calculate curvature are equations derived for **spherical** mirrors. So for a given meridian of the cornea, no matter what the image looks like, the keratometer reads the curvature of a spherical surface that will produce the same size image as the anterior surface of the cornea.

Consider also that the images measured with a keratometer are produced by reflections from two small points on the cornea separated by about 2.5 to 3 mm; the exact separation is dependent on the radius of curvature of the cornea. The shape of the cornea could be altered substantially between these two points without affecting the measurement.

These last two paragraphs point out two of the shortcomings of the keratometer:

1. The readings obtained with the keratometer only reflect curvature for isolated portions of the cornea.
2. The instruments are calibrated for spherical surfaces and they assume that along any given meridian the cornea is also spherical.

CORNEAL POWER READINGS

Keratometers usually provide two different measures of corneal curvature, the radius of curvature and the dioptric refracting power. The radius of curvature is in fact an estimate of the curvature of the front surface of the cornea, but interestingly, the power reading is intended to represent the net dioptric power of the cornea as a whole (i.e. the front and back surfaces together).

How is the total power derived? Assume you obtained a reading of 7.67 mm for the radius of curvature of a patient's eye. The refracting power of the front surface of the cornea can be calculated simply using the formulas for single spherical refracting surfaces.

$$F = \frac{n' - n}{r}$$

F = refracting power
n'= index of the cornea (1.376)
n = index of air (1.0)
r = corneal radius (in meters)

$$F = \frac{1.376 - 1.0}{0.00767 \text{ m}}$$

F = + 49.00 D

However, the power reading of the B & L Keratometer for a 7.67 mm radius of curvature is +44.00 D, i.e. 5.00 D **less** total power than that calculated for the front surface alone. The lower power readings are obtained because the manufacturers have deliberately chosen a lower index of refraction to calculate power to compensate for the fact that the posterior surface of the cornea has a low negative refracting power. The index of refraction used to make these calculations for the B & L Keratometer is 1.3375 (some other commercial instruments use an assumed index of 1.336).

REFRACTIVE POWER OF THE CORNEA

Primarily because the greatest change in index of refraction occurs at the cornea-air interface, the cornea contributes more to the total refracting power of the eye than any other refracting surface (Figure 2.15).

Calculations of Total Power for the 'Average' Cornea

Assume:

Radius anterior cornea = R_a = 7.8 mm
Radius posterior cornea = R_p = 6.8 mm
Corneal refractive index = N_c = 1.376
Aqueous refractive index = N_a = 1.336
Corneal thickness = 0.5 mm

Note: The radius of curvature of the posterior cornea is shorter than that for the anterior surface.

Power of the Front Surface:

$$F_A = \frac{1.376 - 1.0}{0.0078 \text{ m}} = +48.2 \text{ D}$$

Power of the Back Surface:

$$F_p = \frac{1.336 - 1.376}{0.0068 \text{ m}} = -5.88 \text{ D}$$

Equivalent Power of Total Cornea:

$F_{eg} = F_A + F_P - t/n\,(F_A)(F_P)$
$F_{eg} = 48.2\text{ D} - 5.88\text{ D} - [(0.0005\text{ m}/1.376)(48.2\text{ D})(-5.88\text{ D})]$
$F_{eg} = +42.42\text{ D}$

The total power of the unaccommodated eye is approximately +60 D. Since the cornea contributes 60-70% of the total power, it is easy to understand why certain corneal pathologies or defects can have a devastating effect on the eye's refractive status and vision in general.

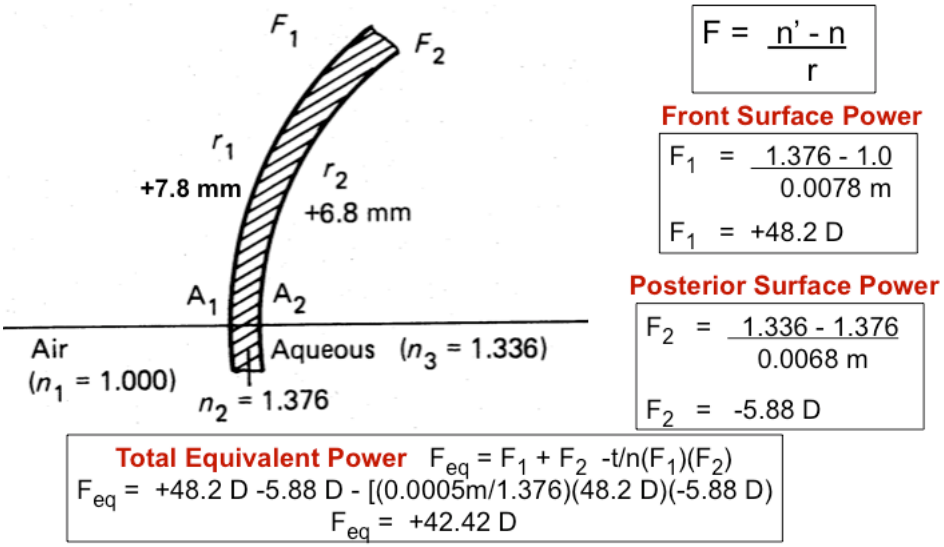

Figure 2.15: *Calculation of total corneal power*

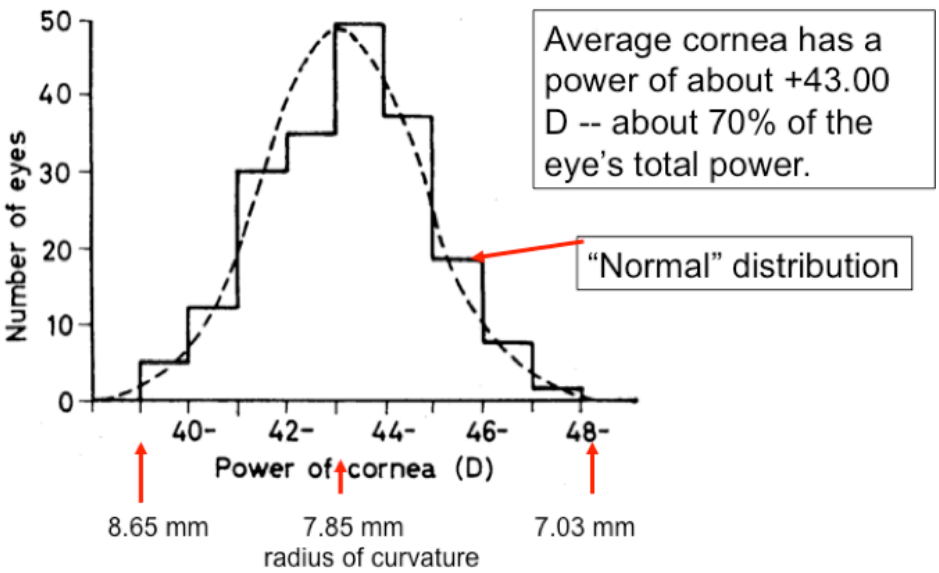

Figure 2.16: *Distribution of Corneal Power in Young Adults*

Note: It should be obvious that light is actually refracted by the tear film before it reaches the cornea proper. When this fact is considered, should one use the refractive index of the tear film rather than that for the cornea proper when calculating the refractive power of the front surface of the cornea? The refractive index of the tear film is generally taken to be about 1.336 which is very similar to the assumed refractive indices chosen by various instrument manufacturers to calculate corneal power. Some texts have argued that that is why manufacturers selected an artificially low refractive index to calculate corneal power. However, the correspondence between the assumed index used to calculate corneal power and the refractive index of the tears is simply fortuitous. One must consider that the tear film is uniformly thick. Therefore, as a separate entity, it actually does not contribute to the net refracting power of the cornea. The tear film can be removed from the cornea without affecting the total power of the cornea (see below).

Now, at the same time, it should be kept in mind that when the tear film is on the cornea, the greatest amount of refraction actually takes place at the surface of the tears. However, because the cornea is behind the tears, the interface between the posterior surface of the tear film and the cornea will have an additional positive refracting effect.

Note: In air, the back surface of the tear film would have a negative power equivalent to the positive power of the front surface of the tear film. In other words, in air the tear film by itself would have essentially zero refracting power, but on the eye both the front and back surfaces of the tear film have a positive refracting effect.

As a result, if you used the refractive index of the tear film (and the radius of curvature of the tear film measured with a keratometer) to calculate the refracting power of the front surface of the cornea, you will underestimate the refracting power of the tear film-anterior cornea combination.

What is the contribution of the tear film, *per se*, to the total dioptric power of the eye?

Assume the following:

Radius anterior cornea	= 7.8 mm
Index of refraction (cornea)	= 1.376
Index of refraction (tears)	= 1.336
Thickness of tear layer	= 10 microns (0.00001 m)

To answer the question we will determine the position of the image of a distant point source formed by refraction at the anterior corneal surface **with** and **without** the tear film.

With tears:

Power of the anterior tear film:

$$F_{(tears)} = \frac{1.336-1.0}{0.0078\text{ m}} = +43.0769\text{ D}$$

Image formed by the anterior tear film:

$$I'_{(tears)} = n'/L' = \frac{1.336}{+43.0769\text{ D}} = 0.0310143$$

Vergence of light at the tear-cornea interface:

$$L = n/l = \frac{1.336}{0.0310043\ \text{m}} = +43.090797\ \text{D}$$

Power of the tear-cornea interface:

$$F_{(\text{ant. cornea})} = \frac{1.376-1.336}{0.0078\ \text{m}} = +5.1282051\ \text{D}$$

Vergence of light leaving tear-cornea interface:

$$L' = L + F = 43.090797 + 5.1282051 = +48.219002\ \text{D}$$

Final image position after leaving the tear-cornea interface:

$$l' = \frac{1.376}{48.219} = 0.0285365\ \text{m}$$

i.e. the image is formed **2.85465 cm** after it hits the tears.

Without tears:

Power of the air-cornea interface:

$$F = \frac{1.376-1.0}{0.0078\ \text{m}} = +48.205128\ \text{D}$$

Final image position after leaving the air-cornea interface:

$$l' = \frac{1.376}{48.205128\ \text{D}} = 0.0285447\ \text{m}$$

i.e. the image is formed 2.85447 cm after it hits the cornea. Hence, the difference in image planes with and without the tear film is an insignificant 0.000182 cm.

Conclusions

1. The tear film, because it is uniformly thick, contributes nothing to the total dioptric power of the eye.
2. Refraction in the normal eye first occurs at the tear film. However, removing the tear film will not (at least from a dioptric stand point) alter the refractive status of the eye.

I have included the above discussion to illustrate the contribution of the tears to refractive power and to emphasize that the power readings obtained from keratometers are intended to represent the **total** refracting power of the cornea, both the front and back surfaces together. As we will discuss later, the posterior surface of the cornea actually has a negative refracting effect.

ACCURACY OF KERATOMETER READINGS

The accuracy of the keratometer is limited by a number of potentially confounding factors including many subject and observer variables (e.g. variations in head position or the direction of fixation; fluctuations in the observer's accommodation). But like any optical device, the accuracy of the keratometer, even under ideal conditions is limited by diffraction. Theoretically, the keratometer cannot provide readings, even on steel balls, with accuracy greater than about ± 0.2 D. When human factors are included, the degree of repeatability gets worse.

For example, one study in which the observer made measurements on steel balls, reported that the range of variability was 0.37 D for horizontal measurements (i.e. ± 0.19 D from the average) and 0.75 D for vertical measurements ± 0.37 D). It is quite likely that measurements of corneal curvature in a clinical setting would be even more variable.

CLINICAL USE OF THE KERATOMETER

When the keratometer was first developed, it had a larger impact in clinical situations than it does today, primarily because its use drew attention to the high prevalence of astigmatism in the general population. Unfortunately, the instrument only measures the astigmatism due to the front surface of the cornea. A substantial amount of clinical data has demonstrated conclusively that astigmatism measured with the keratometer often differs in amount and axis from that determined subjectively. Astigmatic corrections determined subjectively and via the keratometer are in agreement in only about 40% of the cases. However, in general, the higher the amount of corneal toricity, the higher is the agreement. Differences between the keratometric cylinder and the subjective cylinder are attributed primarily to:

1. Lenticular astigmatism and
2. Curvature of the back surface of the cornea

Even when keratometric findings are modified to compensate for the ‘average’ internal astigmatism and lens effectivity (i.e.Javal's rule), keratometers provide only an approximation of the final cylindrical correction.

Due to the differences between the subjective and keratometric astigmatism, the keratometer is not as useful in routine clinical refractions as it is in some special cases. The keratometer is particularly helpful in:

1. Determining the proper base curve for contact lenses (however, with the newer extended-wear, soft contact lenses, its role in contact lens fitting and evaluation is changing)
2. Detecting and monitoring corneal pathology (e.g. keratoconus)
3. Trying to explain poor visual acuities (e.g. distorted mires may indicate abnormal or irregular astigmatism)

4. Determining the nature of a refractive error (i.e. is the refractive error axial or refractive in nature?)
5. Examining patients difficult to manage in a typical subjective refraction (i.e. it is an objective technique that can be used on almost any patient).

It should also be kept in mind that although keratometric findings are not always essential in determining the proper spectacle correction, they are an essential part of the data base for all patients.

CORNEAL CONTOUR MEASUREMENTS

Keratometers used in a conventional manner only estimate curvature for the central part of the cornea. However, it is desirable to know the shape of the whole cornea (i.e. the **topography** of the cornea) for several reasons. First, the fitting characteristics of contact lenses often depend on the relationship between the periphery of the lens and the peripheral corneal contour. And second, accurate knowledge of corneal shape is needed to understand and perform keratorefractive surgery. Consequently, a number of techniques have been developed to evaluate curvature over larger areas of the cornea. (Fig. 2.17).

PERIPHERAL KERATOMETRY

There have been several attempts to use the keratometer to measure corneal contour, however, these measures can at best be considered to represent approximations. To determine corneal contour with a keratometer, a device is attached to the instrument to provide a movable fixation target for the subject. A series of measurements are then made as the patient fixates points that are decentred by a known amount from the optic axis of the keratometer. The accuracy of this method is severely limited by two of the major shortcomings of the keratometer mentioned earlier. The peripheral cornea is definitely not spherical and the curvature changes so rapidly in the periphery that the relatively large separations between the areas of the cornea that reflect the light from the mires cause unusually large measurement errors. Fortunately for measurements of the central cornea, this value corresponds fairly well to the curvature at the corneal apex. However, for the peripheral cornea this error makes the near periphery seem flatter than it really is and the change in curvature at the periphery abnormally large.

SMALL MIRE KERATOMETRY

To reduce the error produced by measurements obtained from widely separated corneal points, investigators have reduced the size of the keratometer's mires. For example, Mandell altered a keratometer so that corneal areas measured were separated by only 1.0 mm. This modification increases the validity of peripheral keratometry. However, obtaining sufficient measurements to provide useful information about the shape of the cornea is very time consuming and as a result is generally not clinically feasible.

PLACIDO DISC

The **Placido disc** or **keratoscopic disc** can be used to assess qualitatively the shape of the cornea. The Placido disc is simply a series of illuminated concentric circles that are imaged on the cornea. The corneal reflex produced by the target is usually viewed through a high plus lens positioned in front of an aperture in the centre of the disc. The plus lens establishes a relatively standard viewing distance and provides positive magnification. The standard Placido disc projects over about 7 mm of the cornea and is generally used to evaluate qualitatively corneal irregularities caused by faulty keratoplasty, keratoconus or corneal scarring. In individuals with a healthy cornea and a low amount of corneal toricity (<3.0 to 4.0 D), the reflected image will be concentric, smooth and basically circular in shape. In individuals with high corneal cylinders, the reflected rings will be elliptical, becoming elongated along the meridian of least curvature.

By itself, the Placido disc is at best a screening device. But since it was introduced, the basic Placido disc pattern has been used in conjunction with a number of other measurement techniques. The most important of these techniques is **photokeratoscopy**.

PHOTOKERATOSCOPY (OR VIDEOKERATOSCOPY)

Photokeratoscopy is a relatively old method (first used by Gullstrand in 1896) for measuring corneal contour and as the name implies it involves photographing the first Purkinje image. The principal used in photokeratoscopy is the same as in keratometry. It involves measuring the size of the reflected image produced by an object of known size and mathematically deriving the corneal curvature using formulas for mirrors. A large Placido disc is usually employed as the object. Therefore, one of the advantages of photokeratoscopy over keratometry is that estimates of corneal curvature can be obtained at a large number of different positions across the cornea. The total corneal area that is measured depends upon the size and shape of the object. Although some investigators have reported that photokeratoscopy has a greater accuracy than the keratometer, there are a number of important sources of error. First, it is difficult to derive a mathematical scheme to obtain the true shape of the cornea. Therefore, just as in keratometry, manufacturers make the assumption that the cornea is either spherical or that it conforms to some other conic section (e.g. an ellipse). Initially, one of the biggest problems in photokeratoscopy was the stability of the film used to produce the photokeratograph. As a result of differences in film shrinkage during development, measurements on steel balls of known radius reveal considerable variability. It has been reported that measurements of radius of curvature are only accurate to within 0.2 mm. However, most commercial videokeratoscopes employ CCD video cameras to digitize the image of the mires reflected from the cornea. With this technology, the image data are undistorted by a photographic process and, more importantly, are immediately available for mathematical manipulations and enhanced computer graphic displays.

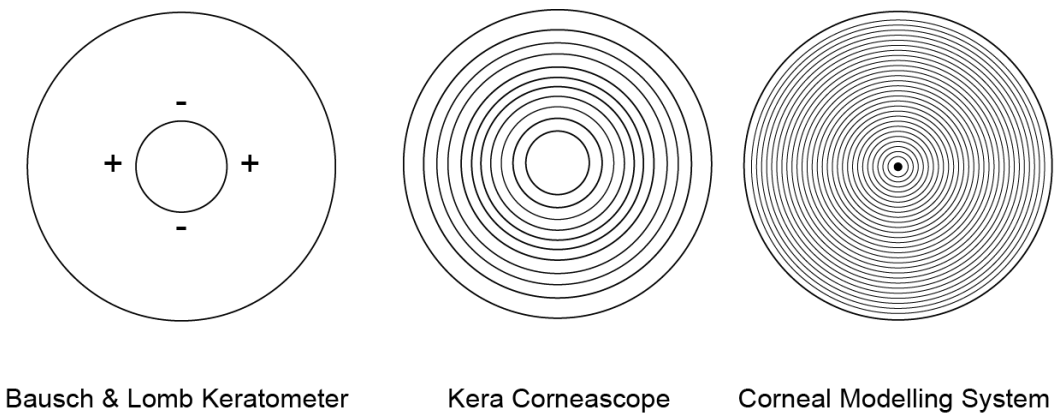

Figure 2.17: *Examples of the mires used as objects in keratometers and videokeratoscopes. Placido or keratocopic disc is a series of illuminated concentric circles that are imaged on the cornea*

OTHER MEASUREMENT TECHNIQUES

Template Measurements

This procedure involves fitting a template of known curvature to either an enlarged photograph of the cornea taken from a lateral position or a solid impression or mold of the cornea. The accuracy of this method is very low because in general it is very difficult to fit templates to small arcs. It is necessary to fit small arcs because the curvature of the cornea is continuously changing. In general, templates can estimate curvature with an accuracy of 2.0 D.

Stereophotogrammetry

With this procedure the cornea is anesthetized, covered with talcum powder, and is photographed from two directions simultaneously using a stereoscopic camera (similar to those used in aerial photography). Very accurate measures of relative height are possible, however, the accuracy of curvature estimates is much lower.

CORNEAL TOPOGRAPHY

QUALITATIVE DESCRIPTION

The cornea as a whole is not spherical. It has an irregular complex shape that cannot be described in simple geometric terms (i.e. it cannot be represented by a conic section). Figure 2.18 summarizes the terminology frequently used in describing corneal shape. It has been consistently demonstrated that the normal cornea becomes progressively flatter in the periphery (i.e. prolate shape; 'positive' shape factor) (Figure 2.19). As a result, the cornea has traditionally been considered to be made up of 3 separate zones, a central, optical,or apical zone (sometimes referred to as the corneal cap), a peripheral zone and a limbal zone. But, no single descriptive scheme is universally accepted. The terminology frequently used by corneal surgeons for describing the anatomic topographic regions of the cornea includes 4 zones, a central optical zone and 3 concentric annular zones (paracentral, peripheral, and limbal zones (Fig. 2.20 and 2.21).

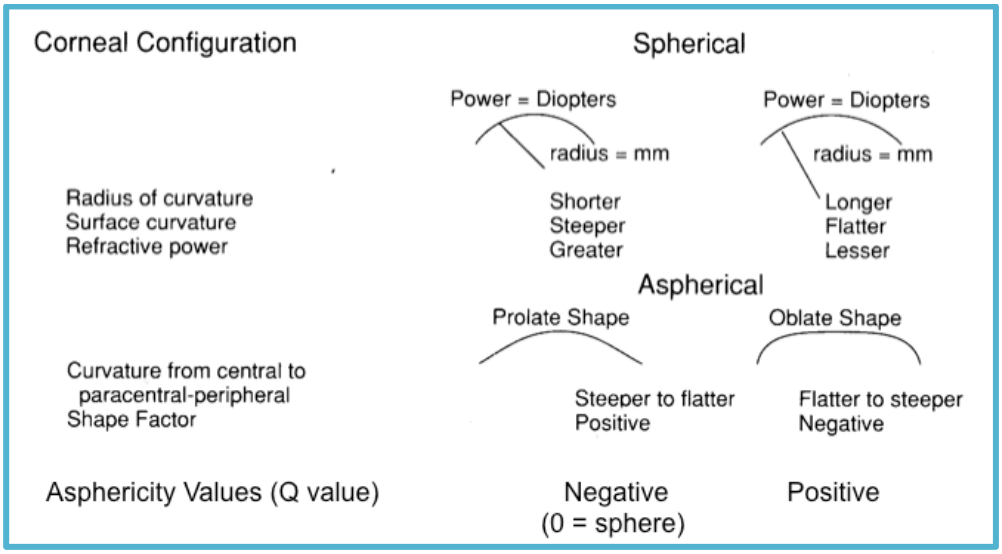

Figure 2.18: *Terminology used to describe corneal shape*

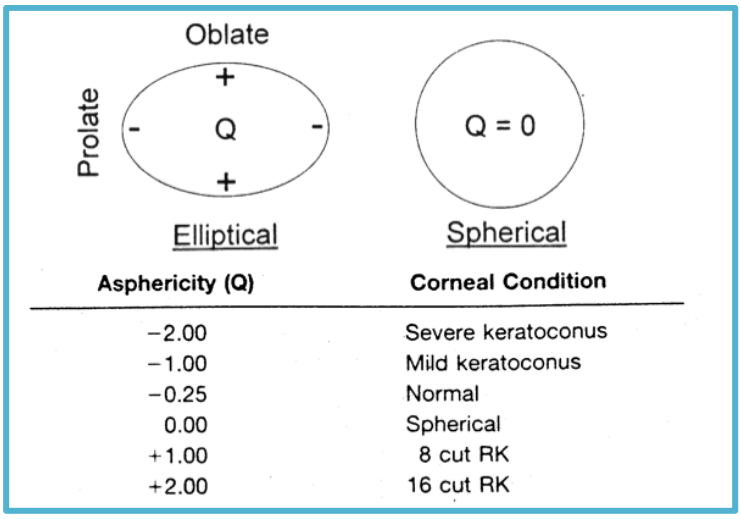

Asphericity (Q)	Corneal Condition
−2.00	Severe keratoconus
−1.00	Mild keratoconus
−0.25	Normal
0.00	Spherical
+1.00	8 cut RK
+2.00	16 cut RK

Figure 2.19: *Asphericity values can be used to describe the corneal shape, which is typically prolate, flatter in the periphery*

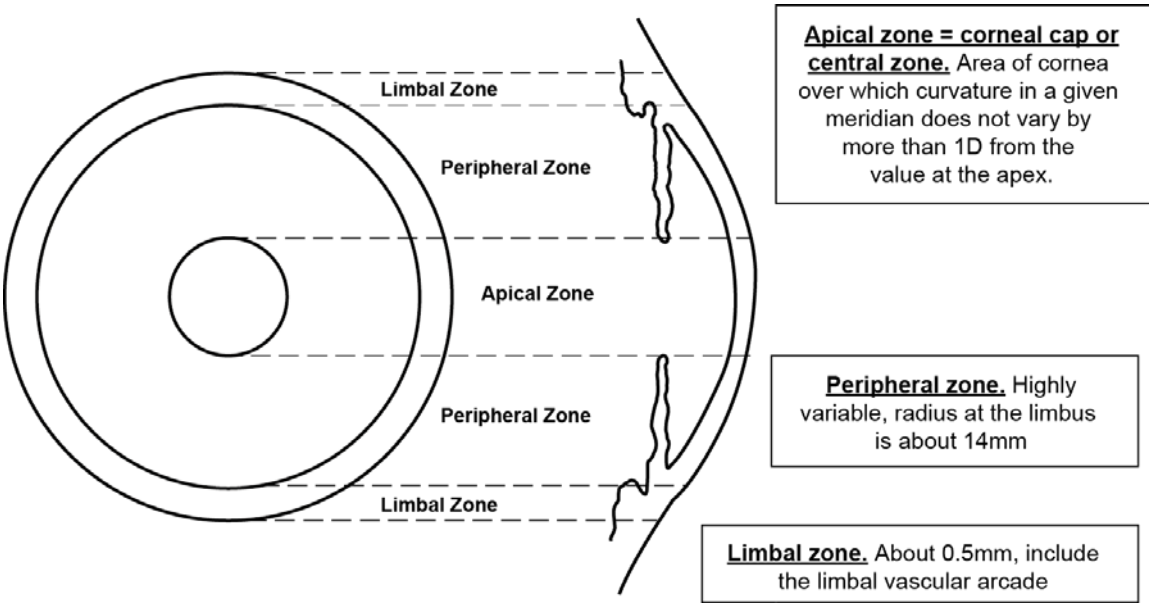

Figure 2.20: *Zones of the cornea*

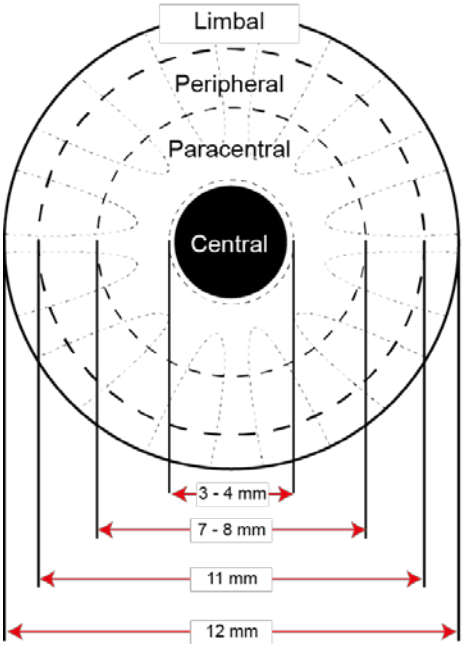

Terminology for describing the anatomic topographic regions of cornea. Typically used by corneal surgeons.

Zone	Approximate Diameter of Region (mm)	Commonly Used Synonyms
Central	4–circle	Optical Zone Spherical Zone Pupillary Zone
Paracentral Peripheral Limbal	4 to 8 annulus 9 to 11 annulus 11.5 to 12 annulus	Mid-peripheral Transitional Far-peripheral
		Apical Zone

Figure 2.21: *Terminology for corneal shape typically used by ophthalmic surgeons*

APICAL ZONE

Classically, the optical zone has been defined as the area of the cornea over which curvature in a given meridian does not vary by more than 1.0 D from the value at the apex (i.e. the point of greatest curvature). The corneal cap is generally considered to be about 4 mm in diameter (range 3-6 mm). Traditionally, the curvature in any given meridian of the cornea has been considered to be approximately spherical within the optical zone, however, most recent texts describe the optical zone as elliptical in shape. The corneal cap or zone of constant radius of curvature actually has a changing radius which changes at a slower rate than the corneal periphery (Figure 2.22).

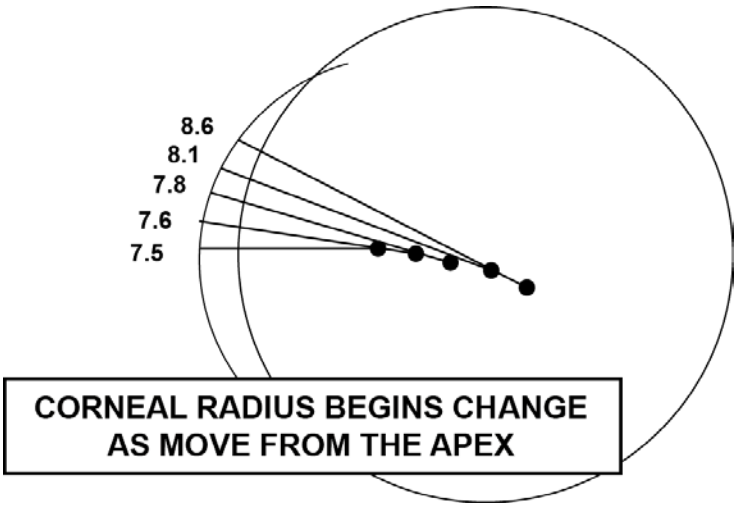

Figure 2.22: *The radius of curvature on the corneal cap actually changes as it moves from the apex of the cornea*

The exact position of the corneal cap (or apex) with respect to the geometrical centre of the cornea varies substantially between individuals. The majority of texts state that the apex of the cornea is displaced down and temporally with respect to the geometric centre of the cornea. But more importantly, the apex of the cornea does not usually coincide with the ophthalmometric pole (the point on the cornea that during normal alignment procedures is transected by the optical axis of the keratometer). When assessing the eye's refractive astigmatism, you would ideally want to align the keratometer with the patient's line of sight. (The intersection of the line of sight and the cornea is sometimes referred to as the 'visual centre' of the cornea.) However, with traditional instruments, there is a small discrepancy between the visual centre and ophthalmometric pole. But even if you did align the instrument with the line of sight, the position of the apex would not typically correspond to the optic axis of the keratometer. A recent study of the position of the apex with respect to the line of sight reports that, for the 1000 eyes studied, the apex was displaced in a temporal direction in 63% of the subjects, in a nasal direction in 16% of the subjects, and it was on the approximate vertical meridian in 21% of the subjects. With respect to the horizontal meridian, the apex was symmetrically distributed about the horizontal meridian. In general, the magnitudes of these displacements are small so that the optical zone is always positioned in front of the pupil. In about 50-60% of the normal population, the corneal apex is within 0.5 mm of the visual centre. Nonetheless, the displacement of the apex from the ophthalmometric pole in the majority of subjects has important implications for keratometry. Since the apex of the cornea is displaced, the mires of the keratometer will not be positioned symmetrically about the apex of the cornea.

The corneal cap is typically toric, i.e. curvature varies systematically from one meridian to the next. In the majority of young adults the cornea's horizontal meridian is the flattest and the vertical meridian is the steepest, a condition referred to as 'with-the-rule' corneal astigmatism. Corneal astigmatism can be irregular, i.e. the meridians of greatest and least power are not oriented 90 deg apart. In fact, for the majority of eyes, a better description of corneal shape is obtained using 4 'semi-meridians' rather than 2 principal meridians. The semi-meridians extend from the limbus and meet at the corneal apex, but they do not meet in a perpendicular manner. Figure 2.23A and 2.23B compares the concept of semi-meridians with that of the traditional cylindrical meridians (note meridians span the diameter of the cornea from limbus to limbus whereas semi-meridians span the distance between the apex and the limbus). But fortunately, for most eyes the principal meridians or 4 semi-meridians are essentially perpendicular or at least can be considered to be perpendicular. The relatively flatter horizontal meridian exhibited by the majority of young adults is thought to be the result of pressure exerted on the cornea by the eyelids. If the eyelids are retracted, it has been observed that there is a shift toward against-the-rule astigmatism that results from a steepening of the horizontal meridian. This observation suggests that eyelid pressure contributes to the high prevalence of with-the-rule corneal astigmatism.

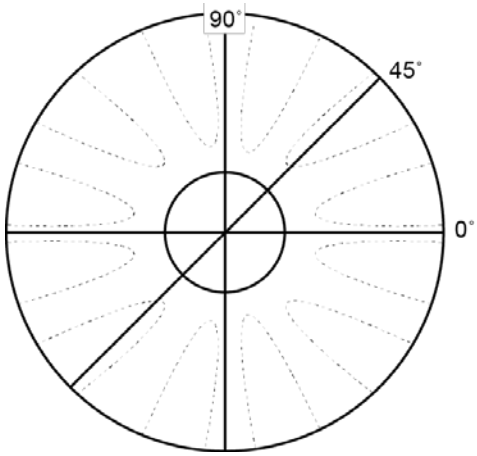

CORNEAL MERIDIANS

Direction of Refractive Power on the Cornea:
Meridians and Axes from 0˚ to 180˚

Meridian: Arc across the cornea from limbus to limbus along which corneal power is measured.

Axis: Orientation of cylindrical lens where there is no refractive power.

Examples of three power meridians or cylindrical axes:

Figure 2.23a: *Corneal meridians and semi-meridians*

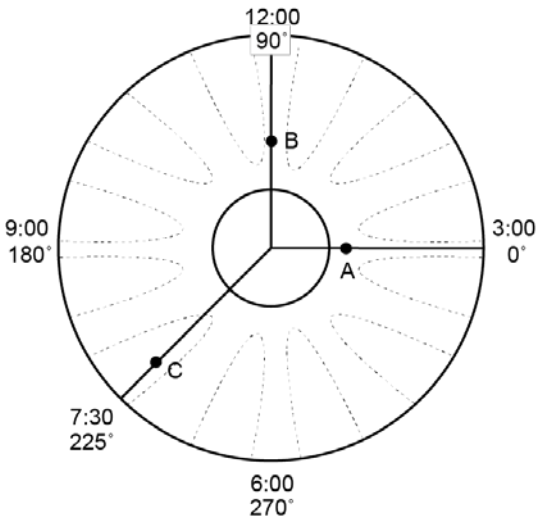

CORNEAL SEMIMERIDIANS

Locations on the Cornea: Semimeridians from 0˚ to 360˚ or from 1:00 o'clock to 12:00 o'clock plus distance from centre of cornea.

Examples of point locations on three semimeridians:

Semimeridian = Centre of cornea to the limbus

Figure 2.23b: *Corneal meridians and semi-meridians*

The radius of curvature of the corneal apex for the 'average' individual is 7.8 mm and the range of values within the normal population extends from about 7.0 to 8.7 mm (about 39.00 to 48.00 D).

PERIPHERAL (INTERMEDIATE) ZONE

The peripheral zone is between the corneal cap and the limbal zone. The shape of the peripheral zone is highly variable. In general, it is believed that the cornea tends to be flatter on the nasal side of the apex than on the temporal side. The radius of curvature of the cornea at the limbus is about 14 mm. The peripheral zone is particularly important when fitting contact lenses because it is the area of the cornea that supports the greatest area of contact with the lens.

LIMBAL ZONE

The junction between the cornea and sclera is the limbal zone. Since the cornea has a steeper curvature than the sclera, an apparent sulcus is formed at the intersection of the cornea and sclera. The limbal zone is about 0.5 mm wide and usually includes the limbal vascular arcade. For the average individual, the diameter of the cornea is approximately 12 mm in the vertical meridian and 13.6 mm in the horizontal meridian. The limbal zone is important because surgical procedures and/or diseases involving this region can have dramatic effects on the shape of the cornea.

MATHEMATICAL DESCRIPTION

It must be emphasized that the division of the cornea into an optical and peripheral zone is highly artificial. For example, in a one study, Mandell reported that only 5 of 26 subjects demonstrated a region of the cornea that remotely resembled a corneal cap (see Fig 2.24). For most individuals, curvature decreases in a relatively regular manner from the apex to the limbus. And if you were to try to describe the shape of the cornea in terms of a simple mathematical expression, it most closely approximates an ellipse. According to Mandell, the central optical part of the cornea conforms closely to an elliptical curve along any given meridian. Significant departures, however, from an ellipse occur in the periphery where the cornea flattens at a faster rate than an ellipse.

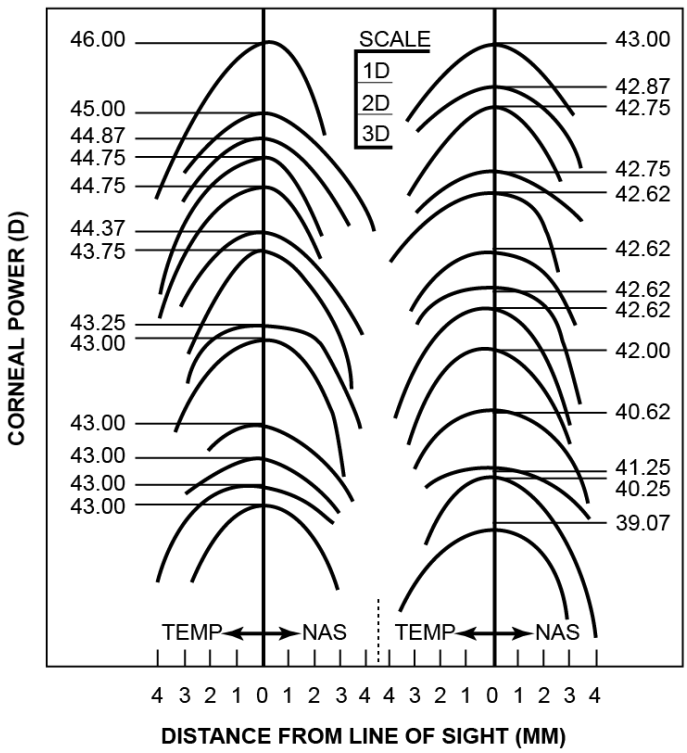

Figure 2.24: *Corneal power profiles of 26 individuals (Mandell)*

Power values for the horizontal meridian measured by small mire keratometry

Division of the cornea into optical and peripheral zones is very artificial. Few individuals have regions of the cornea that resemble a corneal cap.

Each cornea has a unique profile.

POINT-TO-POINT DESCRIPTIONS

The most informative and accurate descriptions of corneal contour are provided by point-to-point representations which consist of an array of corneal power or radius values measured at various positions across the cornea (see Figure 2.25). Videokeratoscopes can provide measures of instantaneous radius at literally thousands of positions across the cornea. One problem with this technique is that it is difficult to take into account all of the information at one time, i.e. it is difficult to get an idea of the corneal contour simply from an array of numbers. The display strategy

that is utilized by most commercially available instruments to overcome this difficulty is analogous to a geographic contour map. Adjacent corneal areas that have similar powers are connected by common colors to form iso-refractive power maps, i.e. contour maps of corneal power, which provide an overall impression of corneal shape.

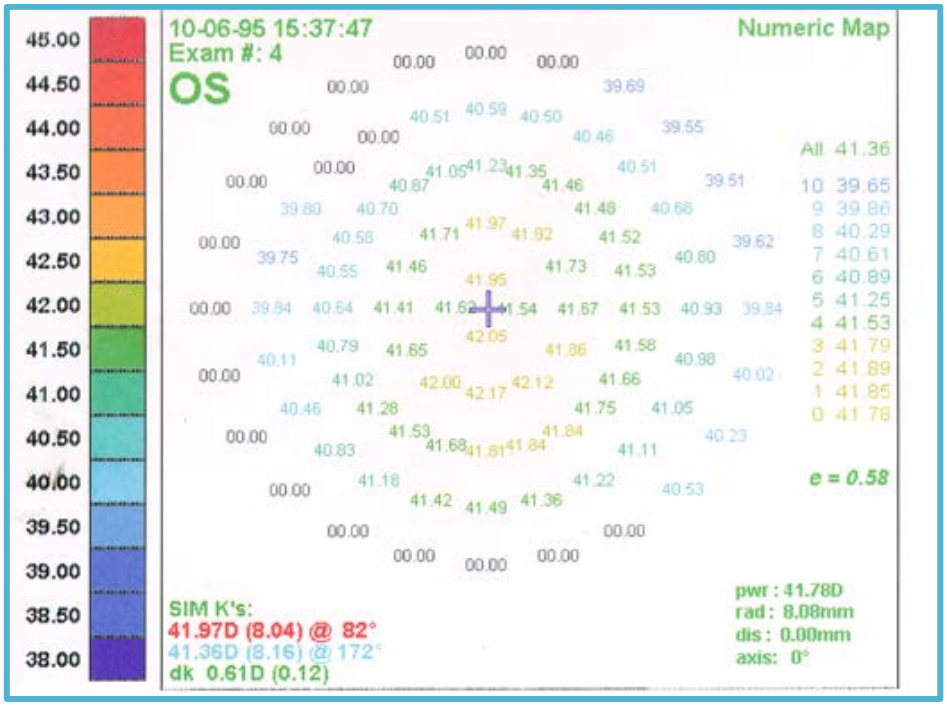

Figure 2.25: *Point to point representation: an array of corneal power readings displayed on a map of the cornea*

Because surface shape is the primary determinant of corneal optics, a logical way to map the corneas is to show the relative surface elevation of each point from a reference surface. Flat references are bad because the minute changes in shape which are optically significant get lost in the larger overall sagittal depth of the cornea. Hence they are usually mapped vs. a reference sphere or ellipsoid (Figure 2.26).

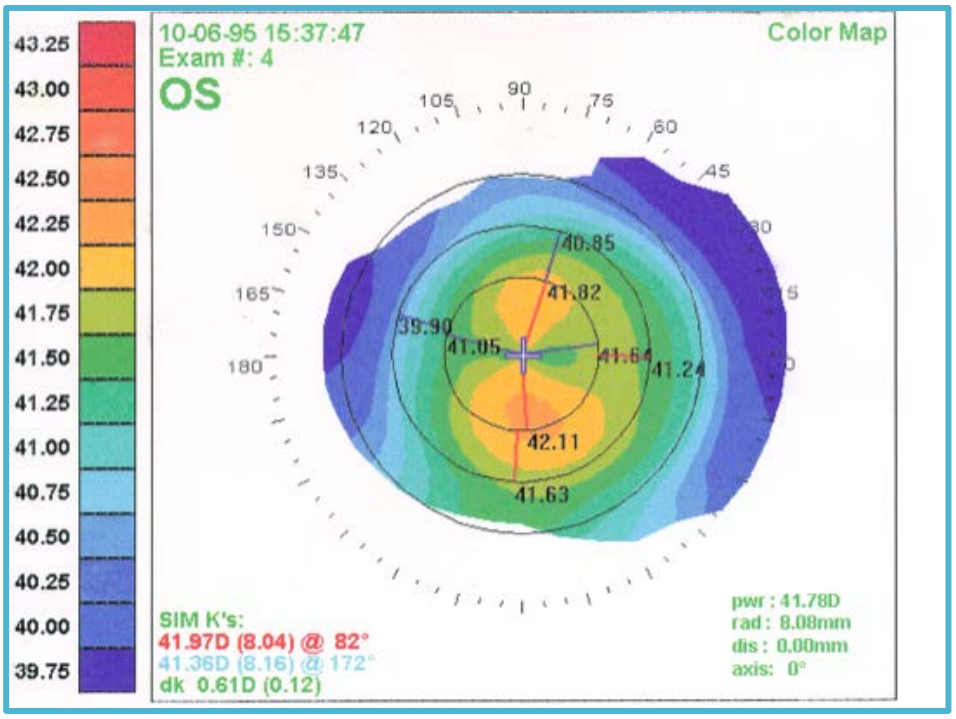

Figure 2.26a: *Colour map showing corneal contours*

To appreciate color power maps, it is important to understand the different ways in which the surface geometry can be expressed in diopters. In topographic maps, the radius measured by the keratometer assumes a centre of curvature on the optical axis, this is sometimes called the sagittal radius. Assuming that the centre of curvature is on the optical axis of spherical surfaces is fine for points near the corneal apex, but big errors occur in the periphery for non-spherical surfaces. Unfortunately, axial radius was the first standard way of representing corneal power. By comparison, instantaneous radius reflects true shape of the corneal surface. This is sometimes called tangential radius or meridional radius (see Figure 2.27).

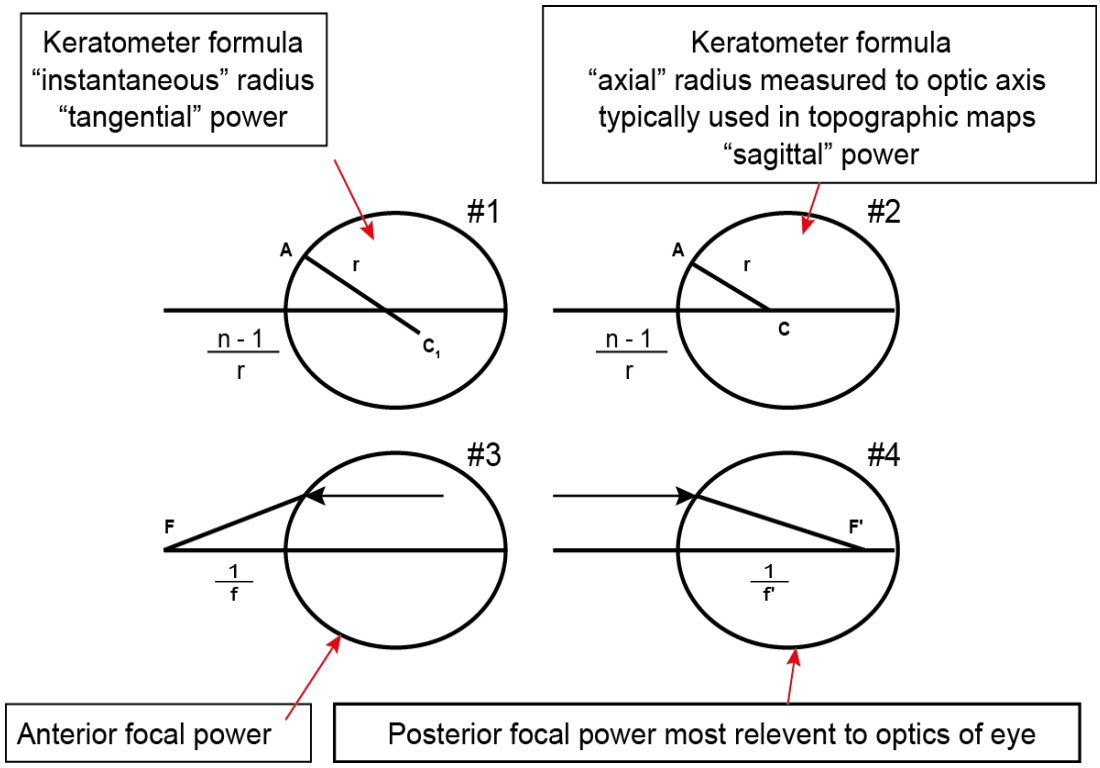

Figure 2.27: *Four different definitions of corneal power and what they represent*

Ray-tracing refractive power maps provide a better way to calculate the refractive power of points across the entire cornea. Basically use Snell’s law to calculate the angle of refraction, the local focal point is determined by where the ray crosses the optical axis (see Figure 2.28).

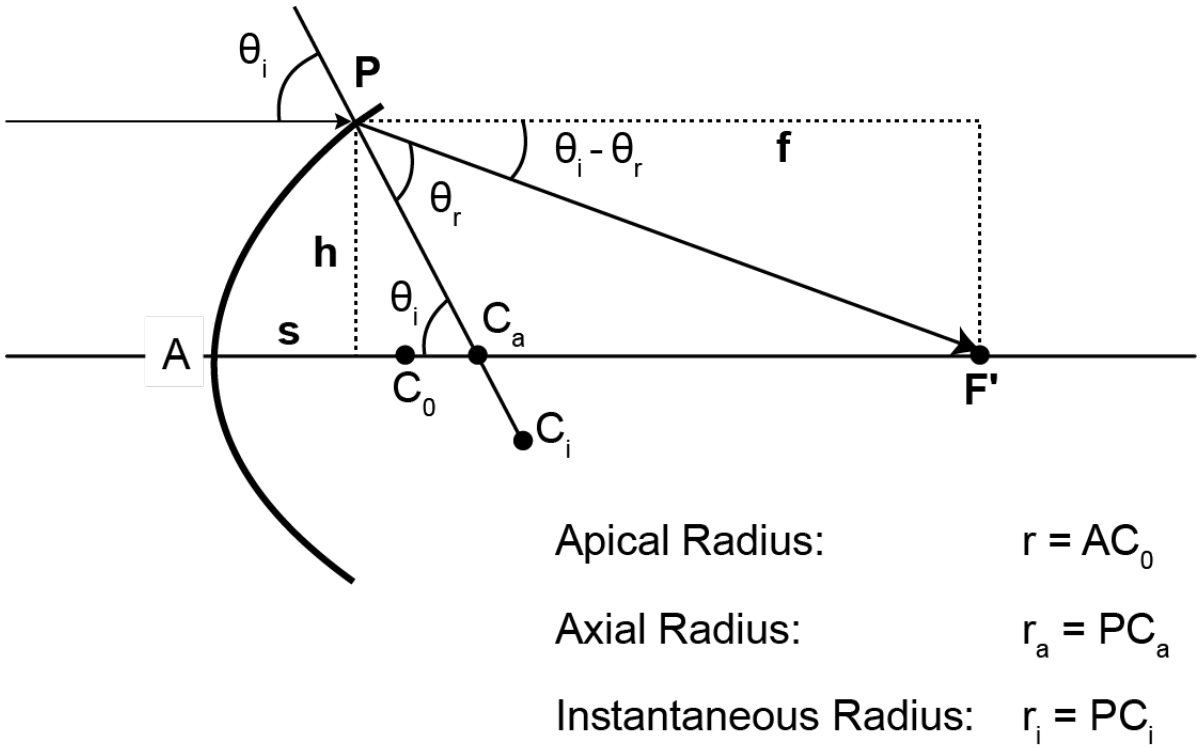

Figure 2.28: *Ray tracing refractive power maps provide a better way to calculate refractive power of points across the entire cornea*

Figure 2.29 provides a comparison of axial and tangential power maps for the same cornea. Both maps have the same apical values and show a decrease in diopters from centre to periphery, indicating a flattening contour. A major difference between axial and instantaneous maps is that instantaneous maps show a greater decrease in dioptric values from centre to periphery. Both maps are based on paraxial optics, where incident light rays are nearly normal to the cornea and hence corneal power is directly proportional to the inverse of the radius. In the peripheral cornea, the angle of incidence from distant parallel rays may be quite oblique, i.e. these dioptric maps do not correctly estimate surface refracting power except near the apex.

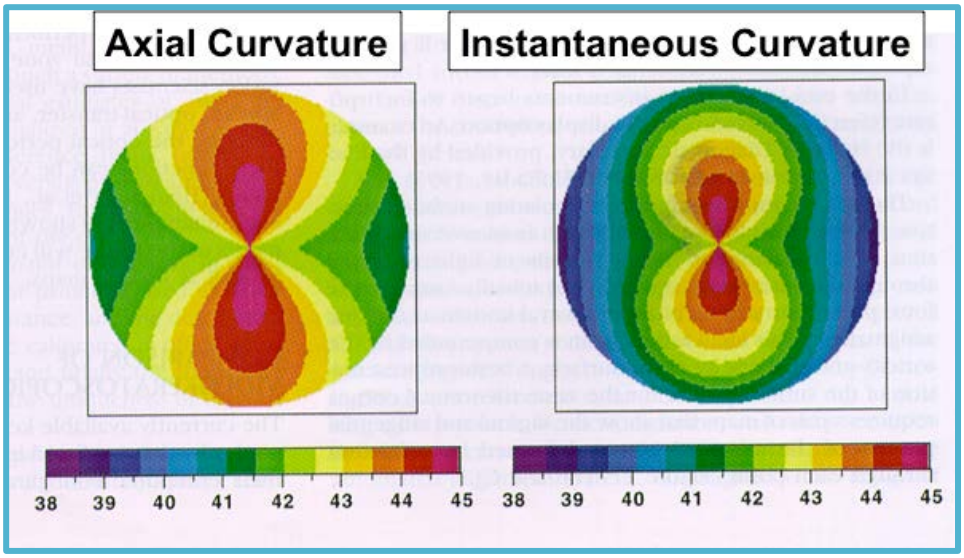

Figure 2.29a: *Comparison of axial and instantaneous power maps for the same cornea*

Note that compared to the dioptric curvature maps of the same cornea, the ray tracing maps are very different (see Figure 2.31). The dumbbell pattern is now oriented horizontally and though the apical values are the same, the ray-

tracing maps show an increase in dioptric values from centre to periphery. This large increase in power occurs because peripheral rays strike the corneas at increasing angles of incidence. This represents spherical aberration of the cornea, a peripheral phenomenon not associated with paraxial optics. Ray tracing maps ignore oblique astigmatism.

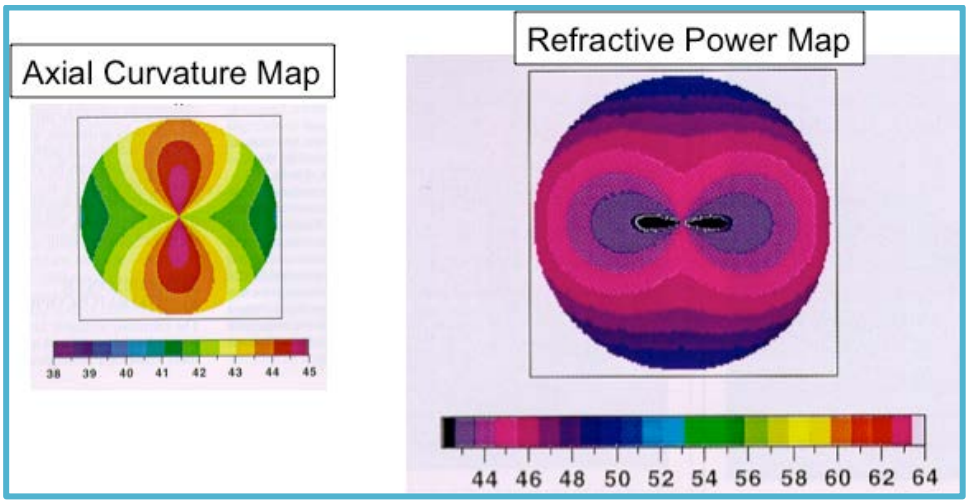

Figure 2.30: *Comparison of an axial curvature map and a ray tracing refractive power map of the same cornea*

Summary of topographic contour maps:

- Surface elevation maps may be particularly useful for monitoring surface anomalies, refractive surgery and custom contact lens fits
- Dioptric curvature maps are most familiar and effectively display changes in local contour…hence useful in monitoring shape
- Instantaneous maps are more sensitive to subtle changes than the axial curvature maps, but they are also more subject to noisy data
- Dioptric curvature maps are not refractive power maps. Dioptric curvature maps show local curvature not true refracting power
- Ray tracing maps show certain optical effects not apparent from any other map, e.g. spherical aberration.

Even with contour maps it is difficult to summarize the shape of the cornea in a simple, brief manner. Recently, investigators have introduced qualitative categorization schemes to help identify and characterize the variability of normal corneal topography. In a study of 399 normal corneas, Waring and his colleagues developed a 5 category classification scheme for corneal topography obtained from color-coded topographic maps. The 5 patterns, which probably represent points along a continuum, are illustrated in Figure 2.31. All the corneas in Waring's sample were steeper centrally and flatter peripherally and the following proportions were classified into each pattern: *round,* 22.6%; *oval,* 20.8%; *symmetric-bow tie,* 17.5%; *asymmetric bow-tie,* 32.1%; and *irregular,* 7.1%. As one might expect from simple inspection of the patterns, oval and round corneas demonstrated less keratometric astigmatism than the bow-tie corneas. However, there were no between group differences in terms of spherical equivalent refractive errors, mean keratometric power, or age of the subject.

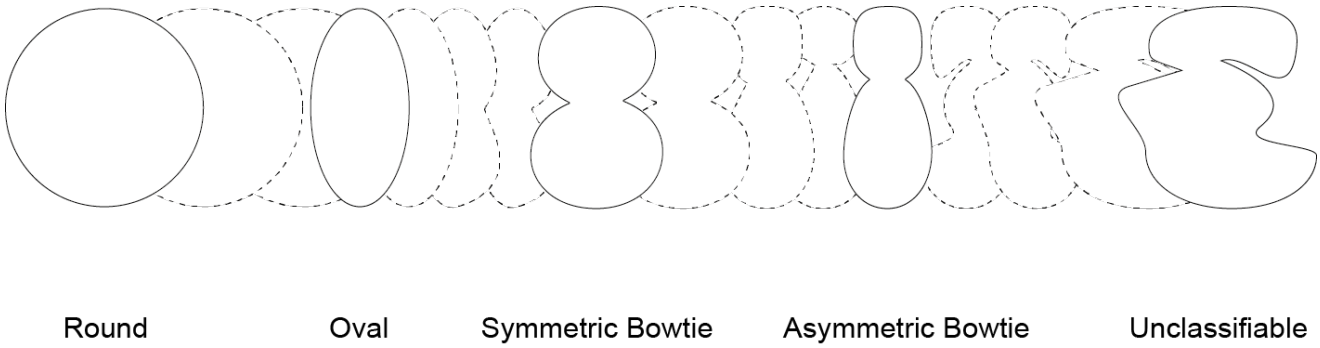

Figure 2.31: *Waring et al described five basic patterns of corneal topography, probably part of a continuum, and labelled them as 'round, oval, symmetric bow-tie, asymmetric bow-tie and irregular'*

Videokeratographic pattern**	Keratometric astigmatism (D)		Refractive astigmatism (D)	
	(mean ± SD)	% ≥ 1.00D	(mean ± SD)	% ≥ 1.00D
Round	0.47 ± 0.34	10%	0.28 ± 0.39	8%
Oval	0.57 ± 0.30	20%	0.26 ± 0.41	7%
Symmetric bow-tie	1.40 ± 0.98	73%	1.00 ± 1.20	43%
Asymmetric bow-tie	0.89 ± 0.70	41%	0.47 ± 0.78	19%
Irregular	0.64 ± 0.53	27%	0.53 ± 0.51	27%

Symmetrical Astigmatism:

Conventional keratometry describes the shape accurately. Note: mirror-image orientation of the astigmatic meridians is a common occurrence which can be clearly demonstrated with photokeratoscopes (see Figures 2.32 and 2.33).

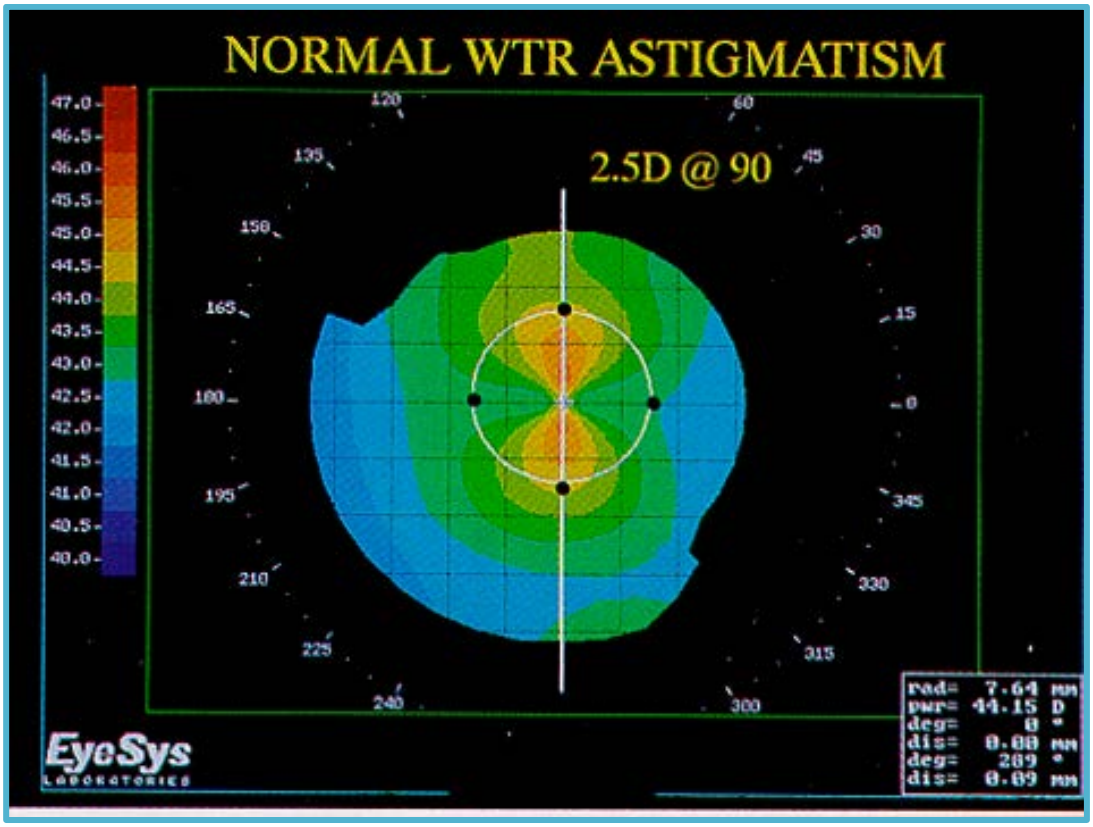

Figure 2.32: *Symmetrical, with the rule astigmatism*

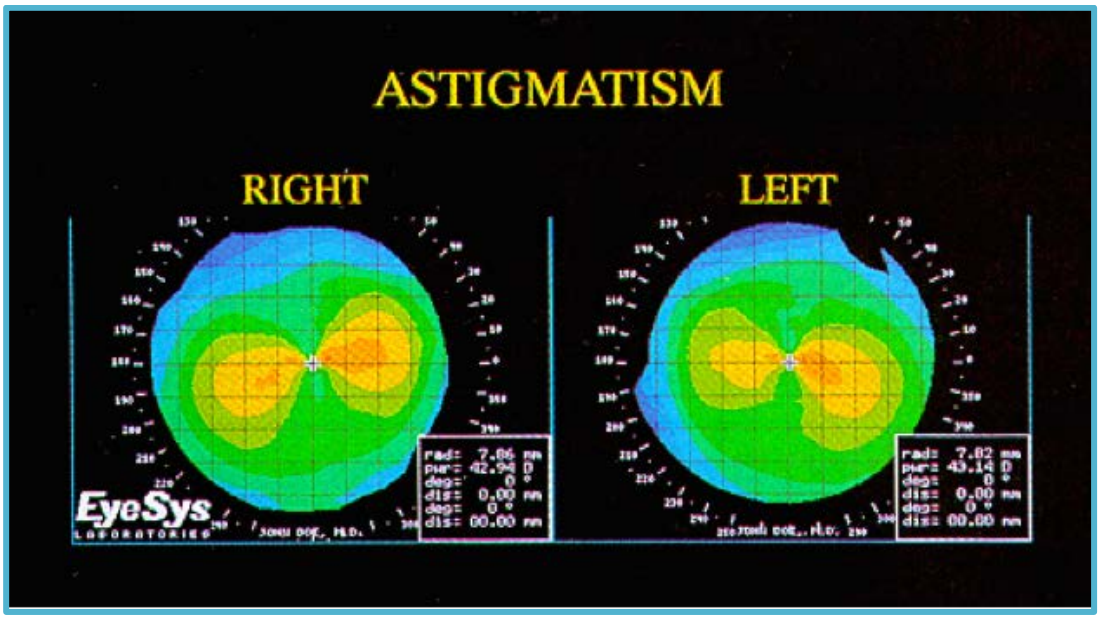

Figure 2.33: *Symmetrical astigmatism showing mirroring of the axis in the right and left eyes*

Asymmetrical Astigmatism:

Corneal topography often provides data that are not apparent from keratometry, even when K readings provide a good estimate of the magnitude of cylinder. For example, you can have different degree of steepening in the superior vs the inferior semi-meridians (Figure 2.34). This information on asymmetrical power changes may be critical in the development of a surgical plan for correcting the patient's refractive error. This information may also be critical in attempting to optically correct individuals after corneal surgery. Corneal topograph can be used to explain apparent discrepancies between keratometric measurements of surgically modified astigmatism and post-operative visual acuity.

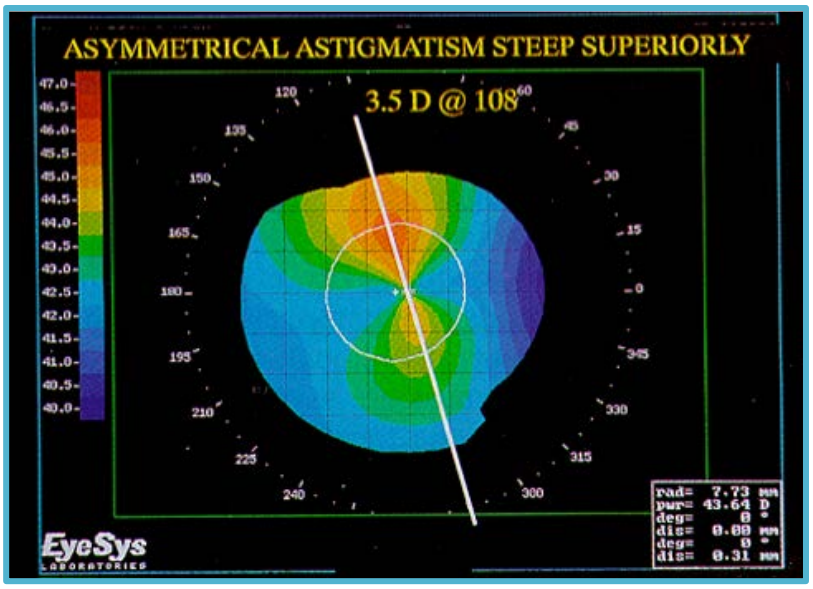

Figure 2.34: *Asymmetrical astigmatism, showing a steep superior cornea*

Whilst conventional keratometry often provides an accurate description of the astigmatism present in a cornea, it does not describe the asymmetry that can be detected with a videotopographer. With the keratomer, the amount and axis of astigmatism is based on the assumption that the cornea is symetrical. For some corneas however, this is misleading when the true topography shows no true astigmatism as in Figure 2.35 and 2.36.

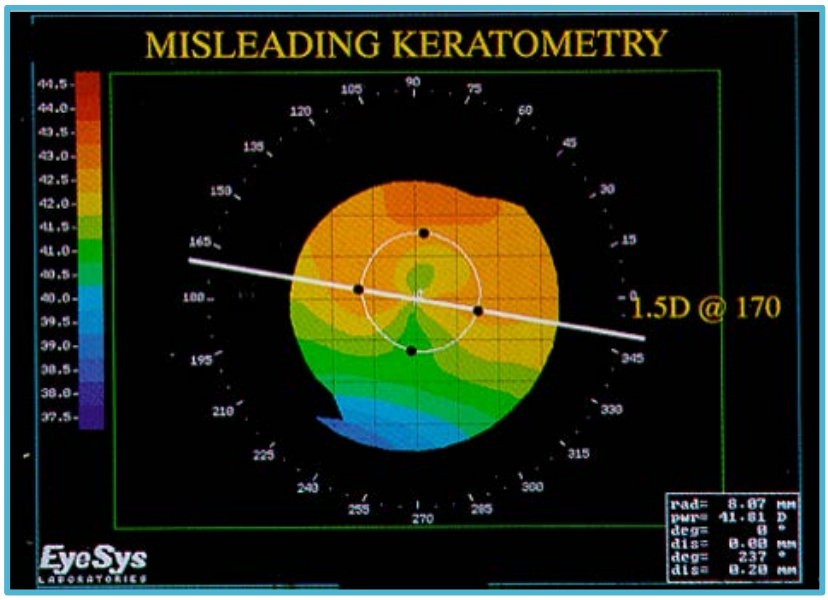

Figure 2.35: *Asymmetric astigmatism*

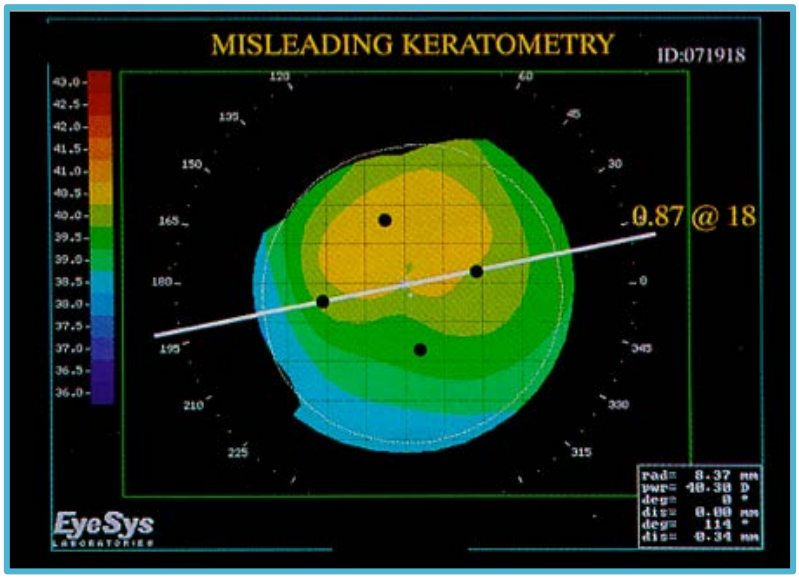

Figure 2.36: *Video topography reveals that the keratometric astigmatism (Indicated by the white line) is not true astigmatism*

4. CURVATURE OF THE SURFACES OF THE LENS: OPHTHALMOPHAKOMETRY

DETERMINATION OF CURVATURES AND POSITIONS OF INTERNAL SURFACES

In order to determine the true radius of curvature for an internal refracting surface, its **apparent position** and **apparent radius** of curvature must be measured (i.e. you must determine the 'equivalent sphere'). Then the true radius can be calculated.

APPARENT RADIUS

One principle used to determine the apparent radius of curvature of a given refracting surface involves measuring the first Purkinje image and comparing it to the size of the Purkinje image produced by the surface in question. For example, to determine the radius of curvature of the anterior surface of the lens, the size of the first Purkinje image produced by a given object would be compared to the size of the third Purkinje image produced by the same object. This comparison would allow you to calculate the apparent radius of the anterior lens surface because, for a distant object, the size of the image formed by reflection at a spherical surface is directly proportional to the radius of curvature. Hence, the relative sizes of the first and third Purkinje images are directly proportional to the **apparent** radii of curvature of the anterior cornea and the anterior lens surfaces, respectively. Therefore, if the sizes of the first and third Purkinje images are known and the **true radius** of curvature for the anterior surface of the cornea can be measured (the apparent radius of the anterior cornea is the true radius since light reflected from the anterior surface is not subsequently refracted), the apparent radius of the anterior lens surface can be calculated using the following relationship:

$$\frac{\text{apparent radius (ant. lens)}}{\text{true radius (ant. cornea)}} = \frac{\text{apparent size of 3rd Purkinje image}}{\text{size of the 1st Purkinje image}}$$

The ratio of the size of any given Purkinje image to the size of the first Purkinje image is proportional to the ratio of the apparent radius of curvature of the surface in question to the radius of curvature of the anterior surface of the cornea.

APPARENT POSITIONS

Tscherning's method of ophthalmophakometry is usually used to determine the apparent radius and apparent position of the internal refracting surfaces. The following description of how Tscherning's ophthalmophakometer can be used to determine the apparent position of the anterior lens surface is included to illustrate the difficulties involved in these indirect measures.

Tscherning's ophthalmophakometer consists of an observation telescope and 2 pairs of movable light sources mounted on a graduated arc perimeter. In order to measure the apparent position of the anterior lens surface (i.e. the depth of the anterior chamber), one light source is positioned on one side of the optical axis of the subject's eye and the telescope on the opposite side. Both are positioned so that the eye's optical axis bisects the angle between the lamp and the telescope. (**Note:** The cornea is assumed to be infinitely thin, i.e. a single spherical refracting surface with its centre of curvature at C. This is a reasonable assumption because the calculated positions of the cornea's principal planes are both very close to the anterior corneal surface.) The telescope is focused for the third Purkinje image produced by light source #1. A vertically oriented pair of light sources (#2) is then moved around the arc until the first Purkinje images produced by these sources are lined up with the third Purkinje image produced by light source #1. B' is the apparent position of the anterior lens surface and the distance AB' (the apparent depth of the anterior chamber) is the distance to be calculated.

Consider the triangle XB'C.

$$\frac{B'C}{CX} = \frac{\sin(\theta)}{\sin(\gamma)}$$

Since CX = the radius of the cornea:

$$B'C = r\,[\sin(\theta)/\sin(\gamma)]$$

The apparent position of the front surface of the lens AB' = r −B'C.

Hence,

$$AB' = r - r\,[\sin(\theta) / \sin(\gamma)]$$
$$AB' = r\,[1 - \sin(\theta) / \sin(\gamma)]$$

The value for r can be determined with a keratometer and the angles θ and γ can be found from the lamp settings. Thus, the apparent depth of the anterior chamber can be calculated using the formula above.

FINCHAM'S TECHNIQUE

Fincham described one of the most direct techniques for determining the apparent position of the internal refracting surfaces. He combined a slit lamp and a corneal microscope. The microscope was fixed to the illumination system so that the microscope was always focused on a specific part of the slit lamp beam. Although the positions of the microscope and the slit lamp were fixed relative to each other, both were mounted on a graduated scale that allowed the lamp-microscope combination to move in the direction of the slit lamp's beam.

To measure the apparent position of a given internal surface the subject is positioned so that the optical axis of his/her eye coincides with the slit lamp beam. The instrument is then adjusted so that the anterior surface of the cornea is in focus and a reading is obtained from the graduated scale. The instrument is then advanced toward the eye until the surface in question (e.g. the anterior surface of the lens) is in focus and another reading is taken from

the graduated scale. Provided that no eye movements occur while the instrument was being adjusted, the difference between the two scale readings is the apparent depth or position of the surface in question.

CALCULATIONS OF THE TRUE RADIUS OF CURVATURE

The following is an example of how the true radius of the anterior surface of the lens is calculated. In order to calculate the true radius of the anterior lens, the apparent radius and apparent position of the lens must first be determined. In addition, to facilitate calculations it is generally assumed that the cornea is a single spherical refracting surface separating air from the aqueous. Assume the following values have been measured:

Apparent lens position = 3.2 mm from the cornea
Apparent lens radius = 15 mm
Radius of the cornea = 7.7 mm
n (aqueous) = 1.336

Imagine A, B, and C represent the true positions of the cornea, anterior lens surface and centre of curvature of the anterior lens, respectively. Point B' represents the apparent position of the lens and B'C' represents the apparent radius of the anterior lens surface (i.e. AB' and B'C' are the values measured for apparent position and apparent radius). BC is the **true radius** of curvature that will be determined by calculating the true position of the lens (AB) and the true position of the centre of curvature (AC).

Points B and B' are conjugate points. B' is the virtual image of B formed by refraction at the cornea. Points C and C' can also be treated as conjugate points. In essence the positions of B' and C' (i.e. the image positions) have been measured and, therefore, the positions of their respective objects, B and C, can be calculated using simple vergence formulas for single spherical refracting surfaces.

First: Calculate the refracting power of the cornea

$$F = \frac{n' - n}{r}$$

$$F = \frac{1.0 - 1.336}{-0.0077 \text{ m}}$$

$$F = +43.6 \text{ D}$$

Note: Object space is the aqueous with an index of 1.336 and image space is air. Following standard sign convention the radius of curvature of the cornea has a negative value since it is measured from the refracting surfaces in the opposite direction of light from the object.

Second: Calculate AB, the object distance for image B'

$$L' = L + F$$
$$L = n/l \quad \text{and} \quad L' = n'/l'$$

Image Vergence:

$$L' = 1/-0.0032 \text{ m}$$
$$L' = -312.5 \text{ D}$$

Object Vergence:

$L = L' - F$
$L = -312.5\ D - 43.6\ D$
$L = -356.1D$

Object Distance:

$l = n/L$
$l = 1.336/-356.1\ D$
$l = -0.00375m$

i.e.the true position of the anterior lens surface (AB) is behind the cornea.

Note: Since the anterior lens surface is the posterior limit of the anterior chamber, AB represents the true depth of the anterior chamber. This example illustrates that the anterior chamber appears to be shallower than it really is (i.e. real depth > apparent depth). The average anterior chamber depth, measured from the anterior cornea, is about 3.47 mm.

Third: Calculate AC, the object distance for image C'

Image Vergence:

$L' = 1 / (-0.0032m - 0.015m)$
$L' = -54.9D$

Object Vergence:

$L = L' - F$
$L = -54.9\ D - 43.6\ D$
$L = -98.5\ D$

Object Distance:

$$l = \frac{(1.336)}{-98.5\ D}$$

$l = -0.01356\ m$

i.e. $AC = -13.56\ mm$

Fourth: Calculate the true radius (BC)

$BC = AC - AB$
$BC = -13.56mm - (-3.75mm)$
$BC = -9.8\ mm$

The true radius of the anterior surface of the lens = 9.8 mm.

Note: Empirically the techniques used to indirectly measure the positions and curvatures of the internal refracting surfaces seem adequate, however, there are a number of obvious errors.

1. All of the measurements are affected by the errors incurred in determining the radius of curvature of the cornea.
2. The cornea is assumed to be spherical and infinitely thin.
3. The internal surfaces are assumed to be spherical.
4. There are a number of inaccuracies involved in measuring the positions and sizes of the Purkinje images.

5. MEASUREMENT OF CORNEAL THICKNESS: PACHYMETRY

Traditionally the only optical constant of the eye's refracting surfaces that was routinely measured in a clinical setting was the radius of curvature of the anterior surface of the cornea. However, for many corneal surgical procedures (e.g. radial keratotomy, photorefractive keratectomy, or LASIK) corneal thickness is a critical parameter that must be taken into account. In addition, some contact lens practitioners have been interested in corneal thickness measurements. With respect to contact lens wear, the interest in corneal thickness stems from the fact that the degree of corneal hydration (the percentage water content) and corneal thickness appear to be directly related. As the water content of the cornea increases, the cornea becomes thicker and it becomes less transparent. Under normal circumstances, the cornea is maintained in a relatively dehydrated state by an energy-dependent metabolic pump. The efficacy of this system to maintain this relatively dehydrated state is dependent on a number of factors, particularly tear osmolarity and oxygen tension. Contact lenses are known to alter these factors, particularly the amount of oxygen available to the cornea. A poor contact lens fit causes the cornea to become edematous (corneal edema is an excessive increase in corneal water content) and, thus, become thicker and less transparent. Typically edema is evaluated qualitatively on the basis of the amount of clouding (reduced corneal transparency) observed with a slit lamp. In this respect, the corneal thickness must increase by approximately 7% before clouding can be detected by slit lamp examination. Some investigators have attempted to evaluate edema quantitatively in terms of the associated changes in corneal thickness. Although there are currently a number of unresolved issues concerning this procedure, corneal thickness measures may also prove to be a valuable index in evaluating the physiological fit of contact lenses.

A **pachymeterpachymeter** is a device that can be used to measure the **apparent** thickness of the cornea. Pachymeters are essentially calibrated doubling devices that attach to the eyepiece of a slit lamp. In the Haig-Strait pachymeter, doubling is produced by two plano glass plates (Figure 2.37). The glass plates are placed one above the other in front of one of the objective lenses of the biomicroscope. Both plates are perpendicular to the optical axis of the microscope. The lower plate is fixed, but the upper plate can be rotated around a vertical axis. As the upper plate is rotated the half image seen through this plate is displaced laterally with respect to the half image viewed through the bottom plate. A scale connected to the moveable plate permits the amount of relative image displacement to be determined. The diagram in Figure 2.38 illustrates how the microscope and the illumination system are positioned to measure corneal thickness (or the apparent anterior chamber depth). The slit lamp microscope is positioned at about a 40° angle with respect to the illumination system. The illumination system is adjusted so that a very thin beam of light is directed perpendicular to the cornea. Ordinarily the illuminated portion of the cornea observed in this manner appears like a cross-section of the cornea (called an optic section). However, when viewed through the pachymeter, the optic section will appear doubled as illustrated below. To measure the apparent corneal thickness, the amount of doubling is first altered to obtain perfect alignment of the two half views. Then in a manner very similar to the doubling procedure used in keratometry, the amount of doubling is varied until the epithelial side of one image is aligned with the endothelial side of the other image. The amount of doubling required provides an indication of the apparent corneal thickness and the true corneal thickness can then be calculated. The average corneal thickness measured with this technique is 0.52 mm (true thickness). This technique can also be used to measure the apparent thickness or depth of corneal features (Figure 2.39).

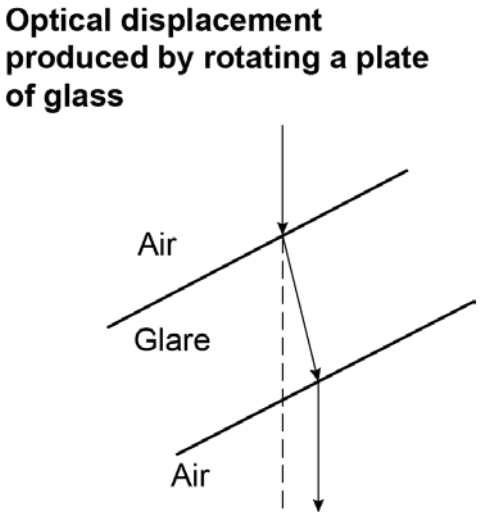

Figure 2.37: *Optical displacement produced by the rotating plate of glass*

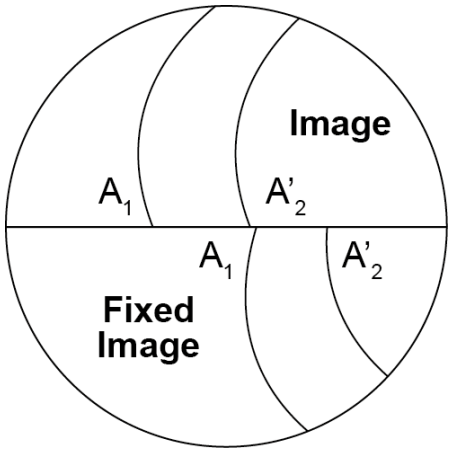

Figure 2.38: *Representation of the doubled corneal section observed*

5. AXIAL LENGTH: X-RAYS AND ULTRASOUND

INTRODUCTION

One of the most important factors in determining the refractive status of an eye is the position of the retina, i.e. the axial length of the eye. Primarily there are two techniques that have been used to measure the axial length of the eye in vivo.

ROENTGENOLOGICAL TECHNIQUE

AXIAL LENGTH

The first technique used to measure axial length was developed by Rhuston. The procedure involves determining the position of the retina with **X-rays** and is sometimes referred to as the roentgenological technique. The technique is based on the fact that when X-rays impinge on the dark-adapted retina they produce **phosphenes**.

Note: Phosphenes are subjective visual sensations produced by non-light stimuli. For example, luminous visual sensations can be produced by stimulating the retina mechanically (mechanical or pressure phosphenes) or with an electric current (electrical phosphenes). The phosphenes produced by X-rays are faint blue in color.

The system consists of a telescope that is adjusted to monitor the position of the anterior pole of the cornea and an X-ray source that generates a very thin sheet of X-rays. The beam of X-rays is parallel to the optical axis of the telescope and both instruments can be moved on a calibrated scale perpendicular to the X-ray beam. The subject is positioned so that the X-ray beam is perpendicular to the visual axis of the eye. Since the X-rays are not refracted by the tissue surrounding the eye, the beam is not deviated from its path perpendicular to the subject's visual axis. Thus, if the sheet of X-rays is projected at the approximate equator of the eye, the beam will produce a circular phosphene. As the X-ray beam is moved backward toward the posterior pole of the eye, the size of the phosphene circle will get smaller and smaller. When the beam is tangent to the posterior pole of the retina, the subject will perceive a small spot instead of a circle.

Subsequent movement of the beam backwards will cause the phosphene to disappear. The objective of the procedure is to determine the plane of the corneal vertex with the telescope and the plane of the posterior pole of the retina with the X-ray beam. The axial length is simply the distance between the telescope and the X-ray beam.

This technique is reported to measure axial length to within 0.2 mm. However, the technique is not used in clinical settings because simpler and safer techniques are readily available. In particular, the operator must be extremely careful that the crystalline lens is not exposed to the X-rays because inadvertent irradiation of the lens can result in cataract formation.

POSITION OF THE NODAL POINT

X-rays and the phosphenes that they produce can also be used to measure the distance between the nodal point and the retina. To determine the position of the nodal point, the large X-ray beam is replaced by two small beams of X-rays positioned one above the other. Again, the two X-ray beams are directed perpendicular to the visual axis of the eye and their positions are adjusted so that both beams intersect the posterior retina. The two beams thus produce two phosphenes one above the other. Since the X-rays are not refracted by ocular tissue the physical separation of the phosphenes will be equal to the physical separation of the two X-ray beams. In essence, the two X-ray beams produce two retinal images separated by a known physical distance. The perceived direction of the two 'images' will be projected out into space through the subject's nodal point. For example, if the subject looks at a screen positioned at a distance, the subject will perceive two blue spots.

Note: Actually there are two nodal points, but they are separated by only about 0.25 mm. So without inducing a substantial error, it can be assumed that the eye has a single nodal point.

By measuring the distance between the two projections (essentially this is the object size required to produce a retinal image equivalent to the separation of the retinal phosphenes) and the distance between the screen and the retina, the distance between the nodal point and the retina can be determined by calculating the altitudes of the two similar triangles. For similar triangles, the ratio of the altitudes is proportional to the ratio of the bases of the triangles (i.e. the ratio of object to image size is equal to the nodal point to object distance divided by the nodal point to retina distance).

TOTAL REFRACTING POWER

In the procedure outlined above for locating the position of the nodal point, if the screen used to measure the distance between the projected phosphenes is at the eye's far point and if the eye is in the unaccommodated state, the total refracting power of the eye can also be determined. When the screen is in focus, the secondary focal point of the eye will coincide with the retina. Therefore, the distance between the nodal point and the retina will equal the distance between the nodal point and the secondary focal point.

Since, $N'F' = -f$

And since $1/-f = F$ (the refracting power of the eye)

$$F = 1/(N'F')$$

ULTRASONOGRAPHY

The most commonly utilised technique to measure intraocular distances in clinical situations (including axial length) is ultrasonography. In addition to measuring intraocular distances, ultrasound has become an important tool because it can be used to detect, outline, and characterize the soft tissue of the eye and orbit, even in the presence of intervening opacities.

Ultrasound is high frequency acoustic energy (sonic vibrations) that is above the range of audible frequencies (about 18,000 to 20,000 Hz and above). The ultrasonic frequencies used to measure ocular distances vary from 1 to 25 meghertz (MHz = million cycles/sec). The higher frequencies have shorter wavelengths and, therefore, provide better spatial resolution than lower frequencies. However, the lower frequencies (and longer wavelengths) penetrate deeper into tissues before the energy is absorbed. The exact frequency used in ophthalmic work depends on the desired measurements. In general, high frequency ultrasound is used for measurements of the anterior segment while lower frequencies are used to determine axial length and for the evaluation of retrobulbar structures.

Although ultrasound is a mechanical energy, it can be reflected and refracted in a manner similar to light. For example, when ultrasound is directed at an interface between two tissues that have different acoustic impedances (acoustic impedance is related to the density of a given media and the transmission velocity of sound in that media), the boundary between the two tissues acts as an acoustic mirror (and an acoustic refracting surface). As a result, some of the ultrasound will be reflected according to the Law of Reflection, i.e. the angle of reflection will be equal to the angle of incidence.

To measure the position of a given interface within the eye, ultrasound is transmitted to the eye from a transducer that contains a **piezoelectric crystal**. Piezoelectric crystals possess 2 important properties. First, the surfaces of these crystals are deformed (thus producing acoustic vibrations) when an electrical current is passed through the material. Second, when acoustic waves strike the crystal, they produce an electrical charge that can be recorded. Thus, if the transducer is positioned in such a manner that the acoustic waves intersect tissue interfaces in the eye in a perpendicular manner, sound is reflected (i.e. an echo) back to the transducer in proportion to the differences in the acoustic impedances of the different tissues. Ultrasound instruments do not continuously emit ultrasound. Instead, a procedure referred to as the ‘pulse-echo’ technique is usually employed. With this technique a brief pulse of sound (typically 1 microsecond in duration) is emitted periodically. Between pulses, the instrument records the time that transpires between when the pulse was emitted and when the returning echo(es) produces a charge on the crystal. The elapsed times can be converted to distances between various interfaces and the probe simply by multiplying the measured time by the velocity of sound in the respective media.

Ultrasound does not travel at a constant velocity in the eye. Instead, it travels faster in the denser structures (e.g. the lens; 1650 m/sec) than it does in the less dense structures (e.g. the vitreous; 1530 m/sec). However, when an ultrasound instrument is used to measure axial length, it is generally assumed that sound travels at a constant velocity in the eye. But in order to take into account the variations in intraocular acoustic velocity, a weighted ‘average’ value for the velocity of sound within the eye is typically employed (e.g. 1540 m/sec). It is important to note that in aphakic patients (i.e. patients without a crystalline lens) it is necessary to assume a slightly lower velocity for sound than that employed with normal patients. Most commercially available ultrasound instruments now include, as an option, alternative operational settings for aphakic individuals.

MODES OF ULTRASOUND

For ophthalmic use, the time between echoes and the strength of the returning echoes are displayed in one of three ways.

A-mode (A-scan, Amplitude mode)

The A-mode is the simplest and most commonly used ultrasound technique. With this technique the strength of the echo produced by a given interface is displayed as a vertical deflection (Y axis) relative to its position (time, X axis) along the path of the ultrasound beam. The strength of the echo, which is related to the angle of the incident sound beam and the differences in acoustic impedance at the interface, is reflected in the height of the display deflection. A normal A-scan echograph obtained when the transducer is aligned with the optical axis is illustrated in Figure 2.39. The deflections associated with the anterior and posterior surfaces of the cornea and lens and the vitreoretinal interface allow measurements of corneal thickness, anterior chamber depth, lens thickness, vitreous chamber depth, and axial length. The aqueous and the vitreous should appear acoustically clear since they are normally homogenous structures.

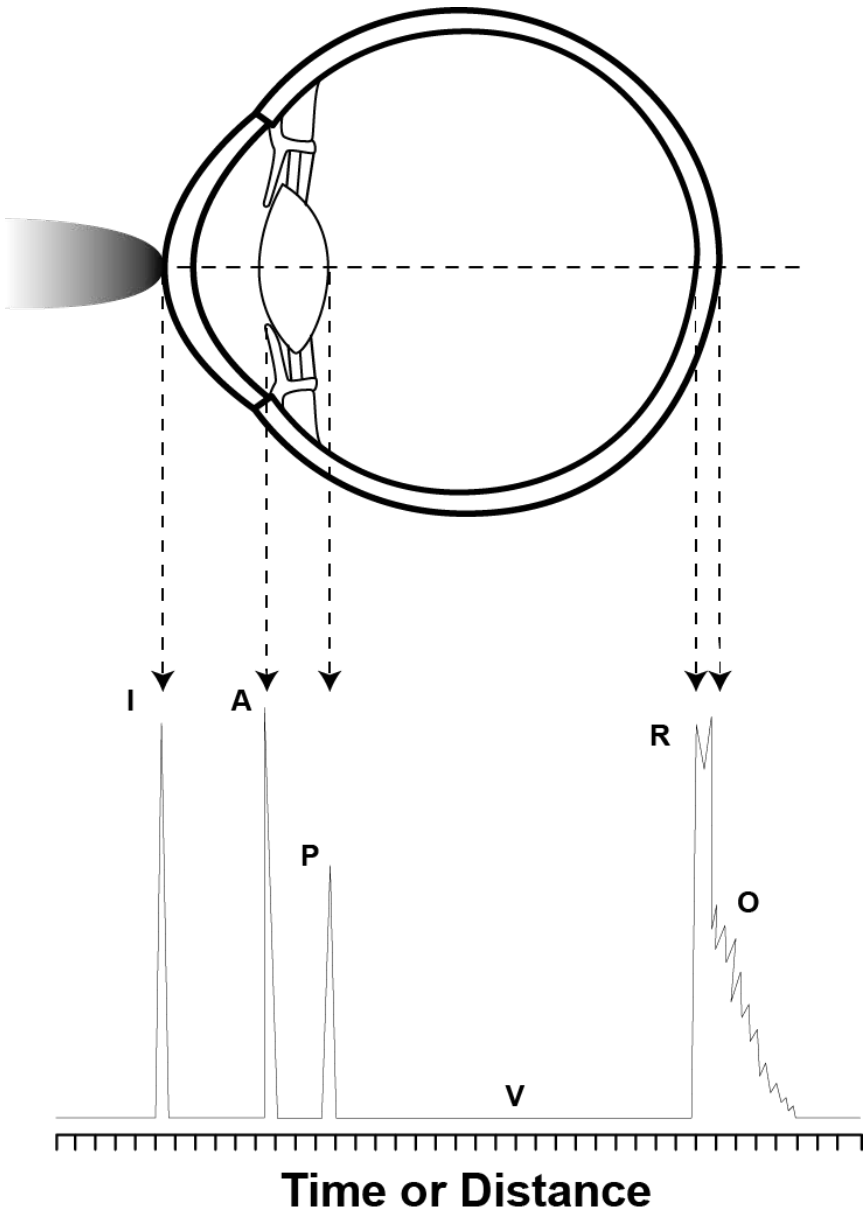

Figure 2.39: *An ultrasound probe on the cornea and the resulting A-scan echograph*

B-mode (B-scan, Brightness mode)

In the B-scan mode, the strength of the returning echo is indicated by an increase in the display brightness as a function of time or distance. In the B-mode, the spatial orientation of the transducer is systematically changed. The transducer orientation and the display orientation are coordinated so that a B-scan echograph looks like a cross section of the globe. Figure 2.40 shows a B-scan obtained along the vertical meridian of a normal eye. In the more sophisticated B-scan systems, the probe is oscillated in 2 dimensions which allows a 3 dimensional echograph of the eye to be constructed.

Although the B-scan is a more involved procedure, it provides the most graphic representation of the relative positions of ocular structures and as a result, it is rapidly overtaking the A-scan as the most commonly utilized display technique. However, in comparison to the A-scan, the B-scan has historically been a much more complicated procedure. For example, instead of simply holding the transducer in contact with the eye or lids (as is typical with the A-scan) an immersion technique was sometimes required. Usually the patient lies on their back and they are fitted with a set of goggles that resemble a scuba diver's mask with the plastic visor removed. The goggles are filled with a saline solution and the probe is placed in the solution. The liquid interface between the probe and the eye allows the probe to be moved (usually by a programmable mechanical device) without losing acoustic contact with the eye. More recently, B-scan probes have been manufactured so that the transducer is completely sealed within the probe (about 1.5 cm in diameter) and rotates about a point inside the probe so that a large scan of the posterior globe is possible simply by placing the probe in direct contact with the patient's lids.

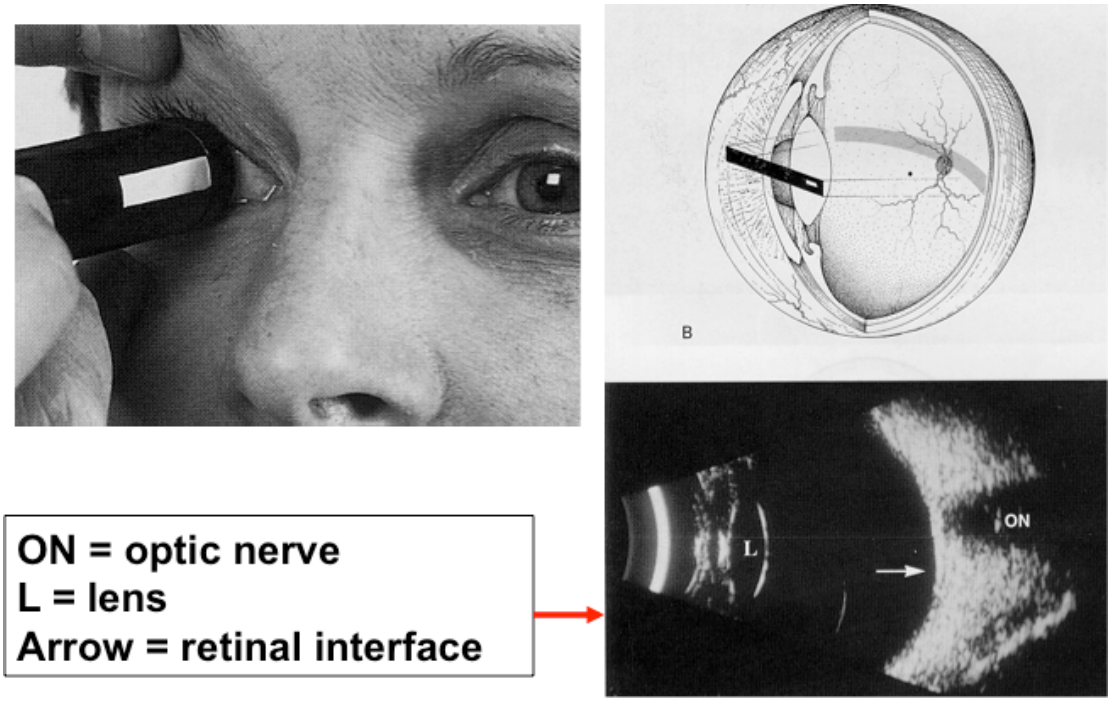

Figure 2.40: *A B-scan along the horizontal meridian*

M-mode (M-scan, Movement mode)

In the M-mode the position and strength of the echoes are displayed as bright dots on the display. However, in contrast to the B-scan, the transducer is held stationary and the oscilloscope display (or film or light sensitive graph paper) is moved in ‘real time’. A typical M-scan is illustrated in Figure 2.41. With this display technique, movement of the tissues associated with accommodation, vascular pressure changes, etc. can be observed over time. It is often used in determining the magnetic properties of intraocular foreign bodies.

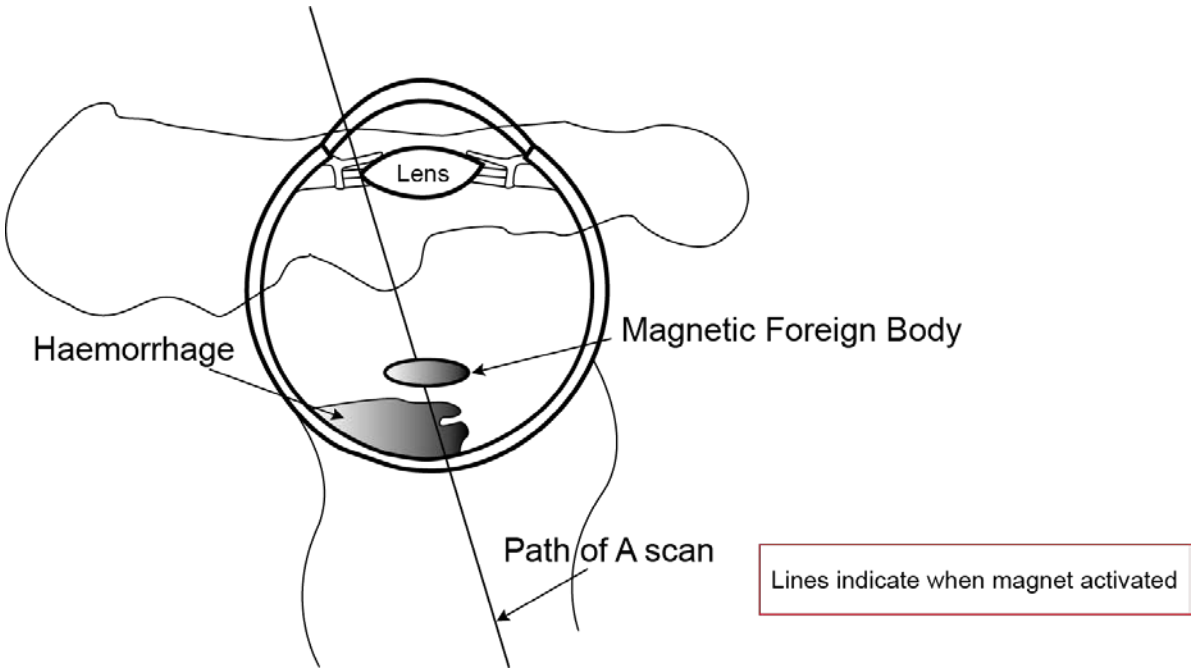

Figure 2.41: *A M-Scan can be used to track the movement of a magnetic foreign body in the eye over time*

CLINICAL USES OF ULTRASOUND

Ultrasound provides an accurate description of normal and abnormal structures even when the structure in question cannot be optically evaluated. The A-mode and B-mode used in conjunction appear to provide the most complete ultrasonic evaluation. The A-mode provides the best means of evaluating the differences in acoustic impedances between tissues while the B-mode provides a two-dimensional view of the eye.

Ultrasound is commonly used to:

1. Locate intraocular foreign bodies,
2. Measure axial length (these measures are particularly critical for determining the proper power for intraocular lens implants) and corneal thickness,
3. Detect and differentiate tumors (for example, solid choroidal tumors can be distinguished from ophthalmoscopically similar lesions filled with fluids),
4. Characterize retinal detachments, and
5. To manage traumatized eyes (the location of hemorrhages can be outlined, the presence of a posterior synechiae and iris bombe can be observed).

BIBLIOGRAPHY

- Krueger SRR, Applegate RA, MacRae M. Wavefront Customized Visual Correction: The Quest for Super Vision. 2nd Edition.Slack, Inc., 2004.
- Duane TD, Tasman W and Jaeger EA. Duane's Clinical Ophthalmology. JB Lippincott Co. Chicago. 2011.
- Tunnacliffe AH.Introduction to Visual Optics.Association of British Dispensing Opticians, 1993.
- Grosvenor TP and flom MC. Refractive Anomalies: research and clinical applications. Butterworth-Heinemann, 1991.
- Atchison DA and Smith G.Optics of the Human Eye, Butterworth/Heinemann, 2000.
- Bennett AG and RabbettsRB. Clinical Visual Optics, 3rd Edition. Elsevier Health Sciences, 1998.